Linköping University Medical Dissertation Nr. 1852

Cell type-specific translatome analysis of mouse models of three genetic neurodegenerative diseases

Susanne Bauer

LINKÖPING UNIVERSITY

Linköping University
Medical Dissertation No. 1852

Cell type-specific translatome analysis of mouse models of three genetic neurodegenerative diseases

Susanne Bauer

Linköping, 2023

Division of Neurobiology
Department of Biomedical and Clinical Sciences
Linköping University, Sweden

Printed by LiU-Tryck, Sweden, 2023

ISBN 978-91-8075-145-2 (Tryckt)
ISBN 978-91-8075-146-9 (PDF)
https://doi.org/10.3384/9789180751469
ISSN 0345-0082

Supervisor
Walker Scot Jackson
Associate Professor
Department of Biomedical and Clinical Sciences
Linköping University, Sweden

Co-supervisor
Martin Hallbeck
Professor
Department of Biomedical and Clinical Sciences
Linköping University, Sweden

Per Hammarström
Professor
Department of Physics, Chemistry and Biology
Linköping University, Sweden

Faculty Opponent
Johan Jakobsson
Professor
Department of Experimental Medical Science
Lund University

Examination Board
Anne Nørremølle
Docent
Department of Cellular and Molecular Medicine
University of Copenhagen

Katarina Kågedal
Associate Professor
Department of Biomedical and Clinical Sciences
Linköping University, Sweden

Giannis Spyrou
Professor
Department of Biomedical and Clinical Sciences
Linköping University, Sweden

Estelle Barbier
Associate Professor, Docent
Department of Biomedical and Clinical Sciences
Linköping University, Sweden

Abstract

The burden neurodegenerative diseases place on patients, their loved ones, and the healthcare system is significant, and despite extensive research efforts, there is currently no cure. Since degenerative changes in the brain can begin years before symptoms appear, early intervention is critical. Additionally, neurodegenerative diseases target certain brain regions and neuron types early on. A more comprehensive understanding of the affected cells during the pre-symptomatic phase is therefore crucial for an effective and targeted intervention.
Herein, we isolated, sequenced, and analyzed translatome samples from six neuronal cell types in knock-in mouse models of three monogenic neurodegenerative diseases at a pre-symptomatic stage: genetic Creutzfeldt-Jakob disease (gCJD), fatal familial insomnia (FFI), and Huntington's disease (HD). To obtain the translatome samples, we used RiboTag to immunoprecipitate HA-tagged ribosomes with their translating mRNAs from targeted cell types. We analyzed six cell types across two brain regions: cerebral and cerebellar glutamatergic and GABAergic neurons, and cerebral parvalbumin (PV) and somatostatin (SST)-expressing neurons.

In the first paper, we focused our analysis on the prion diseases, gCJD (E200K) and FFI (D178N). Here observed a similar response of SST^+ neurons, a cell type not previously reported as affected, in both disease models. This was characterized by upregulation of ribosome-associated genes, and downregulation of cytoskeleton and synapse-associated genes in FFI. Weighted gene co-expression network analysis of SST^+ neurons pointed towards the downregulation of mTOR inhibition as a potential mechanism underlying the observed gene expression changes.

In the second paper, we analyzed a 129S4-HdhQ200 knock-in mouse model of HD. Histological and behavioral assessment revealed pathological changes in the striatum and cerebellum at 9 months and a later, mild behavioral phenotype. Translatome analysis indicated a surprisingly strong response in reportedly resistant glutamatergic neurons of the cerebellum, marked by upregulation of cell cycle regulators *Ccnd1* and chromobox protein genes.

In the third paper, we aimed to compare disease-specific responses of PV^+ neurons across the three disease models. This analysis revealed a milder response in HD compared to prion disease at comparable disease stages. Functional analysis further indicated PV^+ neurons may respond differently in the investigated diseases, showing upregulation of immune response-associated pathways in gCJD, neurodegenerative-disease pathways in FFI, and autophagy in HD.

Lastly, the generation of mouse models such as were used in papers I-III requires stable and predictable transgene expression without interfering with the expression of endogenous genes. In the fourth paper, we conducted a pilot study to compare three potential loci, *Rpl6, Rpl7*, and *Eef1a1*, as potential safe harbors for transgene integration. Preliminary results indicated that the *Rpl6* locus may be best suited for our purposes.

Furthermore, this work generated a novel dataset consisting of translatome profiles of six cell types in three neurodegenerative disease models. This provides gene expression data at a previously unavailable level of cellular resolution, especially in prion disease. We believe that this data will serve as a valuable resource for future research and help expand our understanding of the early molecular mechanisms in neurodegenerative disease beyond the scope of this thesis.

Populärvetenskaplig sammanfattning

Neurodegenerativa sjukdomar som Alzheimers eller Parkinsons sjukdom och även mer sällsynta sjukdomar som Huntingtons sjukdom är ett globalt problem. Diagnosen i sig innebär mycket lidande för både patienter och deras familjer och hittills finns tyvärr inga botemedel. De allra flesta neurodegenerativa sjukdomar orsakas av felveckning av kroppens egna proteiner vilka klumpar ihop sig. Detta påverkar nervcellernas normala funktioner och leder till en progressiv nedbrytning av hjärnceller. Trots att många av de felveckade proteinerna som orsakar dessa sjukdomar finns överallt i kroppen, är det oftast en sjukdomsspecifik typ av hjärncell som påverkas först. Orsaken bakom detta fenomen, som vi kallar selektiv sårbarhet, är dock till största del oklar och förståelse om förändringar som pågår i dessa celler saknas. Dessutom börjar nedbrytningen av nervceller vanligtvis flera år innan patienten visar tecken på sjukdom, som t.ex. försämrad kognitiv- eller rörelseförmåga. För att kunna utveckla effektiva terapeutiska strategier är det därför viktigt att få en bättre förståelse för hur olika hjärnceller förändras. Eftersom det är svårt att undersöker detta hos människor måste vi istället förlita oss på djurmodeller som återskapar sjukdomens huvuddrag.

I den här avhandlingen analyserade vi förändringar i sex olika typer av nervceller i musmodeller av tre genetiska neurodegenerativa sjukdomar innan de visar några symptom. För varje celltyp isolerade vi budbärar-RNA (mRNA), molekyler som instruerar en cell om vilka proteiner den ska tillverka. Sedan analyserade vi skillnader i mRNA nivåer mellan friska individer och de som bär sjukdomsgenen med olika bioinformatiska metoder. Detta gjordes för att förstå hur olika celler förändrar protein som de producerar tidigt i sjukdomsförloppet.

I det första projektet jämförde vi två prionsjukdomar (genetisk Creutzfeldt-Jakobs disease (gCJD) och fatal familial insomnia (FFI)) och såg ett starkt svar i nervceller som uttrycker ett protein kallat somatostatin. Dessa förändringar var också liknande mellan de två sjukdomarna. Trots att den celltypen tidigare visats vara sårbar (i.e. degenererar tidigt i sjukdom) i Alzheimers sjukdom, så fanns det ingen tidigare information för prionsjukdom.
I det andra projektet utförde vi en liknande analys i en modell för Huntingtons sjukdom (HD) där vi observerade det högsta antalet av förändrade gener i en celltyp i lillhjärnan som vanligtvis antas vara resistent. Precis som med det första projektet vet vi ännu inte om dessa tidiga förändringar är ett tecken av sårbarhet. I båda projekten hittade vi de flesta förändringarna i celltyper som inte tidigare rapporterats vara sårbara. Det är möjligt att förändringar som vi upptäckte i dessa hjärnceller är skyddande genom att den tillåter celler att hantera sjukdomen bättre.
I tredje projektet ville vi jämföra förändringar i en typ av hjärnceller som uttrycker proteinet parvalbumin (PV) i CJD, FFI, och HD. PV nervceller upptäcktes vara påverkat tidigt i alla tre sjukdomar, men det fanns hittills ingen celltyp-specifik information om förändringar i genuttryck, särskilt i prionsjukdomar. Vi upptäckte att PV nervceller verkar vara mer påverkade vid prionsjukdomar än Huntingtons sjukdom och kunde identifiera flera sjukdomsspecifika förändringar.
I det fjärde projektet jämförde vi tre olika genomiska regioner för deras lämplighet att generera ytterligare musmodeller.

Sammanfattningsvis upptäckte vi att celltyper som inte tidigare ansågs vara sårbara visade starkaste responsen i våra sjukdomar. Vi kunde identifiera vilka gener som var mest påverkade samt deras associerade molekylära vägar. Men ytterligare forskning är nödvändig för att avgöra om detta är ett tecken på sårbarhet eller en adaptiv förändring.

Vår studie kan bidra till en bättre förståelse av områdes- och celltyp-specifik aktivering av sjukdomsmekanismer i hjärnan, samt om dessa proteiner även är relevanta i ytterligare neurodegenerativa sjukdomar. Dessutom genererade detta en ny offentligt tillgänglig datauppsättning, vilken vi tror kommer bli en värdefull resurs för framtida forskning och kan hjälpa till att utöka vår förståelse av de tidiga molekylära mekanismerna i neurodegenerativa sjukdomar utanför ramen för denna avhandling.

Popular summary

Neurodegenerative diseases, such as Alzheimer's or Parkinson's disease, and even rare diseases like Huntington's disease are a global problem. The diagnosis itself causes a lot of suffering for both patients and their families and unfortunately, there are no cures so far. The vast majority of neurodegenerative diseases are caused by misfolding of the body's own proteins, which can then clump together. This affects the normal functions of nerve cells (neurons) and leads to their progressive breakdown. Although many of the misfolded disease-causing proteins are found everywhere in the body, it is usually a disease-specific type of neuron that is affected first. However, the biological mechanisms behind this phenomenon, which we call selective vulnerability, are still largely unclear, and understanding of the changes that take place in these cells is lacking. In addition, the breakdown of neurons normally begins several years before the patient shows symptoms and is diagnosed. In order to be able to develop effective therapeutic strategies, it is important to gain a better understanding of how different brain cells change. As it is difficult to investigate this in humans, we must instead rely on animal models that replicate the main features of the disease.

In this thesis, we analyzed changes in six different types of neurons in mouse models of three genetic neurodegenerative diseases, before the onset of symptoms. For each cell type, we isolated mRNA, molecules that instruct a cell which proteins to make. We then analyzed differences in mRNA levels between healthy individuals and those carrying the disease gene using different bioinformatical methods. This was done in order to understand how different cells adapt the protein they produce early in disease.

In the first project, we compared two prion diseases (genetic Creutzfeldt-Jakob disease (gCJD) and fatal familial insomnia (FFI)) and found a strong response in neurons that express a protein called somatostatin. These changes were also quite similar between the two diseases. Although that cell type was previously reported to be vulnerable (i.e. degenerate early in disease) in Alzheimer's disease, there was no information on this in prion disease.
In the second project, we performed a similar analysis using a model of Huntington's disease (HD), where we observed the highest number of altered genes in cerebellar neurons that are usually thought to be resistant. As with the first project, we do not yet know if these early changes are a sign of vulnerability. In both projects, we detected the most changes in cell types not previously reported to be vulnerable. It is possible that changes we discovered in these brain cells are protective in that they allow cells to cope better.
In the third project, we wanted to compare changes in a type of brain cells that express the protein parvalbumin (PV) in CJD, FFI, and HD. PV neurons were found to be affected early in all three diseases, but there was so far no cell type-specific information on changes in gene expression, particularly in prion diseases. We discovered that PV neurons appear to be more affected in prion diseases than in Huntington's disease and were able to identify several disease-specific changes.
In the fourth project, we compared three different genomic regions for their suitability to generate additional mouse models.

In summary, we found that in all three diseases, cell types not previously thought to be vulnerable in pre-symptomatic stages showed the strongest response. We were further able to identify which genes were affected and their associated molecular pathways. However, further research is necessary to determine whether this is a sign of vulnerability or an adaptive change.

We think these findings can contribute to a better understanding of area- and cell-type-specific activation of disease mechanisms in the brain, as well as whether these proteins are also relevant in further neurodegenerative diseases. In addition, this generated a new publicly available data set, which we believe will be a valuable resource for future research and can help expand our understanding of the early molecular mechanisms in neurodegenerative disease beyond the scope of this thesis.

List of included papers

I BAUER S, Dittrich L, Kaczmarczyk L, Schleif M, Benfeitas R, Jackson WS
Translatome profiling in fatal familial insomnia implicates TOR signaling in somatostatin neurons
Life Science Alliance, Oct 2022, 5 (11)
doi: 10.26508/lsa.202201530

II BAUER S, Chen CY, Jonson M, Kaczmarczyk L, Magadi SS, Jackson WS
Cerebellar granule neurons induce Cyclin D1 before the onset of motor symptoms in Huntington's disease mice
Acta Neuropathologica Communications, Jan 2023, 11(1)
doi: 10.1186/s40478-022-01500-x

III BAUER S, Jackson WS
Parvalbumin-expressing neurons show disease-specific responses in early stages of neurodegenerative disease
Manuscript

IV BAUER S, Kaczmarczyk L, Jackson WS
Comparative Analysis of Potential Genomic Safe Harbors for Stable Transgene Expression
Manuscript

Relevant abbreviations

CAG	Cytosine-alanine-glycine trinucleotide
CJD	Creutzfeldt-Jakob disease
DEG	Differentially expressed gene
FDR	False discovery rate
FFI	Fatal familial insomnia
GABA	Gamma-Aminobutyric acid
Gad2	Glutamate decarboxylase 2
gCJD	Genetic CJD, here used to refer specifically to gCJD caused by E200K
GO	Gene ontology
GSEA	Gene set enrichment analysis
HA	Hemagglutinin
HD	Huntington's disease
Htt	Huntingtin
ISH	In-situ hybridization
ND	Neurodegenerative disease
ORA	Overrepresentation analysis
polyQ	Poly-glutamine
PrD	Prion disease
Prnp	Prion protein gene
PrP	Prion protein
PV	Parvalbumin
SST	Somatostatin
vGluT2	Vesicular glutamate transporter 2 (also Slc17a6)

Table of Contents

Background

Between 130,000 to 150,000 Swedes are affected by dementia, with one in five octogenarians suffering from the disease[1]. The majority of these cases are caused by neurodegenerative diseases (NDs), such as Alzheimer's and Parkinson's disease, or rarer diseases such as Huntington's disease. Despite extensive research efforts, none of these diseases is currently curable and the development of efficient therapeutic strategies faces several challenges.

One challenge is that, in most NDs, specific brain regions and neuron subtypes exhibit selective vulnerability during the early disease stages, even if the disease-causing protein is expressed ubiquitously[2,3]. For example, striatal projection neurons are the first neurons to degenerate in Huntington's disease[4,5], while in Parkinson's disease, dopaminergic neurons of the substantia nigra show early vulnerability, in Alzheimer's disease noradrenergic neurons of the locus coeruleus are affected early[6], as are alpha motor neurons in ALS[7]. However, the mechanisms and attributes that render specific neurons more susceptible to a given disease are still not well understood.

Secondly, degenerative changes in the brain often begin years or even decades before the overt onset of symptoms[6,8]. Consequently, by the time a diagnosis is made, substantial and irreversible loss of neurons has already occurred. Early therapeutic intervention is therefore crucial, ideally before the onset of symptoms. However, this complicates the study of pre-symptomatic disease mechanisms in humans. Suitable animal models can aid the investigation of pre-symptomatic disease.

Here, we report on studies of knock-in mouse models of three genetic neurodegenerative diseases: genetic Creutzfeldt-Jakob disease (gCJD), fatal familial insomnia (FFI), and Huntington's disease (HD). Although classified as rare diseases, they are each caused by a well-defined mutation in a single protein. Monogenic neurodegenerative diseases, including genetic forms of Alzheimer's disease[9,10], Parkinson's disease, and prion diseases have become popular in scientific research as their study offers several advantages[11]: While differences in clinical symptoms and pathological changes exist between genetic and sporadic forms of the same disease, there is also considerable overlap[12–14], suggesting findings may translate between different disease forms. Furthermore, they are easier to replicate in a disease model than sporadic or polygenic diseases, which have a more complex etiology involving interactions of genetic and environmental factors. Finally, due to having a clear target gene, monogenic diseases are preferred candidates for gene therapy[15,16]. In an ideal scenario, treatments would exclusively aim at affected cells, which necessitates a greater comprehension of the cell type-specific responses within a particular disease, especially during the earliest stages.

In papers I – III, we used the RiboTag method to profile cell type-specific translating mRNAs in knock-in mice modeling gCJD, FFI, and HD at pre-symptomatic disease stages. The overarching aim of this thesis was to investigate cell type-specific responses in early disease, as well as identify central genes and mechanisms that may be interesting candidates as potential therapeutic targets.

Huntington's disease

Huntington's disease (HD) is a fatal, autosomal-dominant neurodegenerative disease caused by the expansion of a cytosine-alanine-glycine (CAG) trinucleotide repeat region in exon 1 of the Huntingtin gene (*HTT*). This mutation results in a poly-glutamine (polyQ) stretch in the Huntingtin protein (HTT). Classified as a rare disease, the incidence of HD is estimated at 6-12/100 000 in Sweden (Socialstryelsen 2023). While HD is mostly known as a movement disorder, cognitive impairment, and behavioral disturbances coincide with motor symptoms or even precede the onset of the motor phenoype[17]. General motor features of the disorder are characterized by initial hyperkinetic symptoms including chorea, involuntary, unrhythmic movements that affect the facial muscles and limbs, and dystonia, repetitive movements caused by involuntary muscle contractions. Chorea usually decreases over the course of disease progression and hypokinesis is more prevalent[18].

Individuals with more than 36 CAG repeats are at risk of developing HD within their lifetime. The age of onset is inversely correlated to the CAG repeat length, although it accounts only for approximately 60% of the variability. Increasing evidence points towards the length of uninterrupted CAG repeats, rather than the length of the polyQ stretch, driving the age of onset since the effect on disease onset is lost if other glutamine-encoding codons (such as CAA) are interspersed[19]. The remaining variance shows heritability[20], suggesting the existence of other genetic modifiers. GWAS studies in over 9000 HD patients have identified potential modifiers that may impact the age of onset, including components of the DNA mismatch repair system *Msh3 (*MutS Homolog 3*), Mlh1* (MutL Homolog 1)*, Mlh3* (MutL Homolog 3), and DNA repair nuclease *Fan1* (FANCD2 and FANCI Associated Nuclease 1)[21,22]. This points towards a central role of DNA repair and maintenance mechanisms in HD onset, potentially by affecting somatic CAG expansion[23]. The expanded trinucleotide repeat is unstable and has been shown to expand in postmitotic neurons, resulting in mosaicism in the brain. This somatic expansion is more prevalent in vulnerable brain regions i.e. striatum and cerebral cortex[24], suggesting it may be a contributing factor to HD pathology in addition to being a modifier of age on onset[25].

The huntingtin protein (HTT)

The molecular changes underlying HD are not fully understood but likely occur due to a combination of both, gain-of-toxic-function effects of the mutant HTT (mHTT) protein by CAG expansion, and the loss-of-function of the wild-type protein. Wild-type HTT encodes for a ubiquitously expressed 348-kDa protein, which has been shown to physically interact with over 350 different proteins[26], supporting its proposed role as a scaffolding protein, and is consequently involved in a variety of cellular processes.

HTT interacts dynein, kinesin, and dynactin, either directly or via the Huntingtin-associated protein 1 (HAP1), facilitating the intracellular trafficking of vesicles and organelles, and through its interaction with dynein is involved in proper positioning of mitotic spindle poles. It is further proposed to be involved in the regulation of endocytic vesicle fission, endosomal trafficking, and induction of autophagy (reviewed here[27]). HTT also interacts with several transcription factors or regulators modulating the transcription of neuronal genes and

neurotrophic factors, such as the neuronal survival factor brain-derived neurotrophic factor (BDNF)[28]. Wild-type HTT further binds and sequesters the RE1-silencing transcription factor (REST)[28], itself a repressor of various neuronal genes including BDNF, enhances CREB-mediated transcriptional activation of neuronal genes. HTT also interacts with and enhances the methyltransferase activity of the polycomb repressor complex 2 (PRC2)[29], a key epigenetic silencer repressing transcription of genes through di- and tri-methylation of histone H3 (H3K27me3) during neuronal differentiation, and is thus involved in the regulation of chromatin remodeling. PRC2 deficiency in adult striatal neurons results in changed transcriptional profiles, characterized by upregulation of developmental genes, such as homeobox genes and cell death-promoting genes, and downregulation of cell type-specific marker genes[30]. Strikingly, PRC2 deficiency mimics changes commonly observed in HD[31,32] and results in progressive degeneration of neurons[30]. This supports the notion that transcriptional changes as a result of improper gene silencing through PRC2 deficiency contribute to HD pathology.

Early attempts to develop total knock-out mouse models have led to the discovery that deletion of HTT is embryonic lethal around E7.5-8.5[33,34], suggesting HTT is essential during development. Indeed, several neurodevelopmental effects have been identified in HD, including aberrations in fetal cortical development that results in a thinner cortex[35], aberrant striatal development[36], and reduced head circumference in carriers of mHTT which are evident decades before the estimated onset of disease symptoms[37]. Studies into the mechanistic role of HTT indicated that it is essential for the proper formation and orientation of mitotic spindles[38], synaptic connectivity[39], the formation of apical junction during cortical development[35], and the determination of cell fate[40], among other processes. Further supporting the idea that loss-of-function of wild-type HTT is a contributing factor in the changes in brain architecture and function observed in carriers of mHTT prior to disease onset.

Neuropathology

HD is characterized by the early and selective vulnerability of GABAergic medium-sized spiny neurons (MSNs, also referred to as spiny projection neurons) which account for approximately 95% percent of striatal neurons. They can be differentiated by the expression of dopamine receptor subtypes, D1 and D2. D2-expressing MSN of the indirect pathway are affected and degenerate earlier in disease than D1-MSN[41], although the mechanisms underlying the different vulnerabilities of these subtypes are not clear.

A hallmark of HD neuropathology is the presence of neuronal intranuclear inclusions (NIIs) and cytoplasmic aggregations which contain aggregated mHTT. While these are often present before the onset of symptoms, their appearance and location do not correlate well with cellular dysfunction or degeneration, suggesting that the formation of inclusion bodies is beneficial rather than pathogenic and that diffuse mHTT oligomers form the principal toxic species[42,43].

Neuropathology is best described in the striatum and the Vonsattel grading system[8] used to rate the severity of HD is heavily based on the degree of striatal degeneration. However, the striatum is far from the only region showing pathology in the form of neuronal loss and astrogliosis. Other affected brain regions include the cerebral cortex, hippocampus, thalamic

nuclei, brainstem nuclei, and the cerebellum and widespread pathology and reduced volumes can be observed in several regions in early and mid-stage HD[39,44–46].

Molecular Pathology

Early and progressive transcriptional changes are well-documented in HD. Reduced expression of striatal-enriched genes (*Drd1a, Drd2, Adora2a, Penk, Ppp1r1b*) are among the most consistently reported early changes[31,32,47,48]. Importantly, several of these genes are also reduced in response to PRC2 deficiency[30].

Analysis of gene expression changes in bulk striatal tissue indicated that even in pre-symptomatic disease, transcription, RNA metabolism, cell cycle, mitochondrial function, and adhesion are affected[47,49]. D2-MSN, and to a lesser extent D1-MSN, account for the majority of gene expression changes observed in bulk striatum of Q175 mice[47,48]. Aberrant expression of mitochondrial genes is commonly reported and altered energy metabolism is thought to be a major contributing factor to HD pathology. A recent study[48] comparing transcriptional changes of D1 and D2 MSN subtypes in HD knock-in mice indicated the release of mitochondrial RNA (mtRNA) and subsequent activation of immune response in SPNs. This study further demonstrated that while both types showed considerable overlap in DEGs and downregulation of synapse and circadian entrainment-associated genes, D2-MSNs showed more pronounced transcriptional changes in early disease. Interestingly, oxidative phosphorylation pathway genes were upregulated in D1-MSN and downregulated in D2-MSN in the knock-in model but downregulated in both MSN types in the more aggressive R6/2. This led to the hypothesis that the upregulation might be an adaptive response of more resistant D1 MSNs.

The cerebellum in HD

While the basal ganglia are the primary site of pathology in HD, there is evidence for early involvement of the cerebellum, although in general, cerebellar pathology is more variable compared to other brain regions[45,50,51]. Intriguingly, it appears the presence and extent of cerebellar pathology in HD patients are not correlated with striatal degeneration or CAG repeat length[45,51]. Cerebellar pathology in HD is predominantly defined by a loss of GABAergic Purkinje cells, the primary output cells of the cerebellum, and general atrophy, while glutamatergic neurons in the granular layer appear comparatively spared[45,51–54].

Although the exact involvement of the cerebellum in HD symptoms is not completely understood, its critical role in motor coordination, balance, posture, cognitive function, and emotional regulation, suggests that its contribution could be a significant factor in the development and progression of HD. A recent study found that cerebellar degeneration is significant in patients with a motor-dominant phenotype, but not in patients presenting behavioral disturbances as initial symptoms[51]. Moreover, cerebellar phenotypes such as ataxia may be underreported in HD[55]. Discovery of the existence of anatomical connections between the cerebellum and basal ganglia (reviewed here:[56]), and findings of increased functional connectivity between the striatum and cerebellum in asymptomatic children with extended

CAG repeats[36] have given rise to the hypothesis of cerebellar compensation. This hypothesis posits that the cerebellum may be able to compensate for the loss of striatal function in the early stages of HD[36,57] and that therefore, the onset of symptoms in HD may be driven, in part, by a loss of cerebellar compensation. While this hypothesis is not universally accepted, it underscores the need for a better understanding of cerebellar pathology and its involvement in HD.

Prion diseases

Prion diseases (PrDs) are a group of fatal neurodegenerative diseases caused by infectious, misfolded species of prion protein (PrP) that can cause a variety of phenotypically different diseases that present with distinct clinical symptoms, incubation periods, and neuropathological changes.

PrDs are separated into sporadic, acquired, and genetic forms. In the vast majority of human PrD cases, the disease occurs spontaneously, with sporadic CJD (sCJD) estimated to account for 85-90% of cases. Acquired PrDs result from the transmission of misfolded PrP species between individuals, for example through the consumption of infected tissue (e.g., ritual cannibalism in Kuru or consumption of contaminated beef in variant CJD), exposure to contaminated medical equipment (iatrogenic CJD), or in the case of animal diseases scrapie and chronic wasting disease, through contact with infected animals or environmental contamination. In contrast, genetic PrDs (gCJD, FFI, and Gerstmann-Straeussler-Scheinker syndrome) are caused by the inheritance of autosomal dominant mutations in the prion protein gene (PRNP) and account for approximately 10-15% of prion disease cases in humans. In this thesis, we have investigated mouse models for genetic CJD and FFI, and will therefore focus on these specific diseases in the following sections.

The prion protein

The cellular prion protein (PrP^c) is an evolutionarily conserved protein with a flexible tail at the N terminus and a C-terminal globular domain consisting of three α-helices and two β-sheets that is attached to the external side of the cell membrane with a GPI anchor. PrDs are characterized by a conformational change of the cellular form to the aggregation-prone, infectious PrP^{sc}, which acts as a template for the misfolding of PrP^c.

The physiological function of endogenous PrP^c is still highly contested. In contrast to Huntingtin, *Prnp* null mutants are viable and a variety of *Prnp* knock-out models have been generated[58–60]. However, these mice show diverse phenotypic variations, which has led to a variety unrelated of roles being attributed to PrP^c, including involvement in phagocytosis of apoptotic cells[61], involvement in synaptic function[62,63], and myelin homeostatsis[64]. It was later found that several of these effects may instead originate from genes flanking the *Prnp* locus and co-segregating with *Prnp.* Such is the case for the gene encoding the signal regulatory protein α (*Sirpa)*, a flanking gene involved in the regulation of phagocytosis, a function

previously misattributed to *Prnp*[65]. This discovery may explain some of the variation in *Prnp* functions observed across various studies and mouse models. As of now, the endogenous role of PrP^{c} remains elusive.

An important genetic determinant in PrDs is the polymorphism at codon 129 of *Prnp*, which can result in a methionine (M) or valine (V) at this position. Homozygous individuals with the MM or VV genotype are overrepresented in sporadic and acquired PrD cases[66], while heterozygosity (MV) seems to confer some resistance. The distribution varies between populations. In Northern Europe (Finland, Denmark, UK, Ireland) the distribution in the normal population is 35-49% homozygotes for M/M, 42-56% heterozygotes, and 9-17% homozygotes for V/V[67,68]. In genetic prion disease, the 129 polymorphism has been shown to influence the disease phenotype, in particular in cases caused by the D178N mutation, but it is under dispute whether it modifies the age of onset[69].

Genetic Creutzfeldt-Jakob disease

The first identified mutation associated with gCJD was a glutamic acid (E) to lysine (K) substitution at codon 200, with methionine at codon 129M (E200K-129M)[70]. While more than 20 mutations have been identified since, the E200K substitution is the most common form of gCJD identified worldwide[71]. The age of onset is highly variable, ranging from 33 to 84 years, with an average of 60.4 years in European cases[72]. Patients with the 129M/V genotype show a slightly extended disease duration[73]. A systematic study of European patients found the most reported initial symptoms were fast-progressing dementia, ataxia (> 80% of cases), followed by myoclonus (> 50%), while pyramidal signs and dystonia were reported in about a third of cases[73]. Insomnia has been reported in some patients with the E200K (~8%)[73], which is consistent with PET scans indicating thalamic hypometabolism[74,75]. This is in clear contrast to the clinical symptoms associated with sporadic CJD and is reminiscent of FFI, described in more detail below.

Neuropathology

A hallmark of gCJD is the presence of spongiosis i.e., the emergence of holes in brain tissue of affected regions that result in a sponge-like appearance. Additional disease-typical changes are neuronal loss, pronounced astrogliosis, and the presence of proteinase-K resistant PrP deposits (PrP^{res})[73]. In E200K gCJD, the cortex, in particular deeper layers, show early vulnerability and atrophy. Cortical pathology is consistently characterized by spongiform degeneration, neuronal loss, PrP^{res} deposits, and reactive astrogliosis with little variation between MM or MV cases. Besides the cortex, more variable lesions and PrP deposit patterns can be seen in the caudate, putamen, and thalamic nuclei[73]. Neuropathology in the cerebellum is also highly variable. Here, the presence of diffuse or synaptic PrP^{res} is associated with spongiosis and neuronal loss, which, in contrast, is absent in CJD cases showing stripe-like deposits of PrP^{res} in the molecular layer that resemble the branching of Purkinje cells[73].

Fatal familial insomnia

FFI was first clinically described as a distinct disease in an Italian family in 1986 by Lugaresi et. al.[76]. So far, only one disease-causing mutation has been identified: the aspartic acid (D) to asparagine (N) substitution at codon 178 in combination with methionine at codon 129 of the mutated allele (D178N-129M)[77]. The polymorphic codon 129 is particularly critical in FFI, as the D178N mutation in combination with 129V instead results in a CJD phenotype[78,79]. As with gCJD, the age of onset varies drastically between cases, ranging from 19 to 83 years, with a slightly lower average age of 51.2 years[72]. Currently, around 50 affected families have been identified world-wide[80]. The 129 polymorphism of the non-mutated allele also appears to have a disease-modifying effect, with heterozygous patients (129M/V) showing prolonged survival (26 months, compared to an average of 9 months in 129 homozygotes)[81] and a more pronounced motor phenotype[82,83].

Clinically, FFI is characterized by rapidly worsening insomnia that is not ameliorated by sedatives and is often accompanied by vivid dreams. While insomnia is a common and prominent symptom, it can be absent. Additionally, patients also present with progressive autonomic dysfunction such as hypertension, sweating, dysregulation of body temperature, hyperhidrosis, tachycardia, and weight loss[82–84]. Psychiatric symptoms and cognitive impairment, including dementia, and hallucinations are also frequently reported[80,82]. Overall, there is considerable heterogeneity in clinical presentation between geographical clusters[82].

Neuropathology

The mediodorsal and anterior ventral thalamic nuclei, as well as the inferior olives, are consistently affected in FFI, showing early vulnerability marked by neuronal loss and extensive astrogliosis[78,82,83,85], while the presence of activated microglia is more variable[85,86]. Other affected brain regions include the hippocampus, cortex, and cerebellum. These are initially relatively spared and show more variable pathology in later disease stages[81,85]. In general, spongiform degeneration and proteinase K-resistant aggregates -the typical neuropathological features of CJD- are mostly absent in FFI[83], although spongiosis and PrP^{res} granular deposits have occasionally been recorded in cases with extended disease duration[84] or in the entorhinal cortex[85]. In the cerebellum, neuropathology is characterized by selective loss of parvalbumin-expressing Purkinje cells and astrogliosis[85]. MRI and PET studies in heterozygous patients showed atrophy of the cerebrum and cerebellum with pronounced hypometabolism in the thalamus, that extended to additional brain regions[83].

Molecular pathology

Post-mortem studies on molecular pathology in human FFI patients from China[87] and Spain[88] (all 129M/M) indicate that mitochondrial function, transcription regulation, protein synthesis, and protein folding are among the most significantly affected pathways in the thalamus. Indeed, expression levels of subunits of all five electron transport chain complexes were found to be reduced at the mRNA or protein level[87,88]. While this is consistent with observed hypometabolism in this region, the reduced expression levels were likely due to severe loss of thalamic neurons (80-90%) at the investigated stage[88]. Reports on changes in PRNP mRNA

expression levels vary: one study[85] reported reduced expression of PRNP mRNA in the thalamus and entorhinal cortex, whereas a second study found no changes[87].
A comparison of gene expression between the thalamus and the mildly affected parietal lobe indicated that electron transport chain-associated genes were differentially expressed in both regions, although the parietal lobe was generally much less affected[87]. In addition to mitochondrial function, protein synthesis was also consistently reported to be altered in the thalamus (and to a much lesser extent in the parietal lobe)[87,88], although this was not always reflected at the mRNA level[88]. Proteomic analysis of FFI showed neurodegenerative disease and oxidative phosphorylation pathways were among the most significantly affected in the cerebellum[89].

In summary, gCJD and FFI manifest as distinct diseases, affecting different brain regions, and with distinct clinical symptoms and neuropathology. However, there is currently a severe lack of data on gene expression changes for both diseases. A challenge is their overall rareness, which makes it exceedingly difficult to obtain large-scale datasets. Consequently, findings are usually based on the investigation of a few samples (publications cited here had sample sizes ranging from 3 to 8 individuals in the disease group). Additionally, for studies conducted on human samples, it is also important to consider that these findings are based on the investigation of post-mortem tissue and therefore reflect terminal disease stages. Furthermore, variability in handling and delays in the processing of tissue samples is an issue in human post-mortem samples and can lead to reduced RNA quality.

Targeted cell types

In papers I-III, we focused on targeting two subpopulations of GABAergic neurons, namely PV and SST-expressing neurons in addition to broader populations of inhibitory and excitatory neurons (Fig. 1). To target general populations of excitatory neurons, we used a vGluT2-ires-Cre driver line[90]. The vesicular glutamate transporter isoform 2 (vGluT2, also Slc17a6), is one of three isoforms expressed in the CNS. Of these, vGluT1 and vGluT2 appear to mostly target separate populations in the adult brain, with vGluT1 more dominant in the upper cortical layers and hippocampus, and vGluT2 in subcortical structures, including the thalamus, midbrain, and medulla. However, there is clear evidence of neurons (transiently) co-expressing both vGluT1 and vGluT2 or switching expression during development including in the hippocampus[91] and in cerebellar granule neurons[92]. Thus, while the use of a vGluT2 driver line does not result in the expression of RiboTag in all glutamatergic neurons, it allowed us to target critical population in the thalamus, cortex, and cerebellum. Using a constitutively expressing Cre driver thus ensured RiboTag activation also in cerebellar granule cells.

Inhibitory, GABAergic neurons were targeted using a Gad2-ires-Cre driver line. *Gad2* encodes for the glutamic acid decarboxylase Gad65, which catalyzes the synthesis of GABA, resulting in the expression of Cre throughout development[93].

GABAergic interneurons form a heterogenous group of inhibitory neurons that are commonly categorized into three subgroups based on their expression of markers: parvalbumin (PV), somatostatin (SST), or serotonin receptor 5HT3a (with or without co-expression of vasoactive intestinal peptide). These groups can be further subdivided by their morphology, location, targets, and electrophysiological properties[94,95]. Inhibitory interneurons play a critical role in modulating and integrating the excitatory and inhibitory signals in neuronal circuits and are thus central for many higher-order functions impacted in neurodegenerative diseases, such as cognition and memory[96,97], sleep[98,99], or motor function[100].

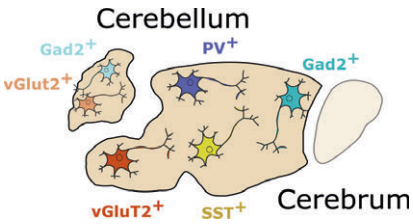

Figure 1: Targeted cell types for papers I-III. For each disease model, we analyzed translatome from six cell types. In the cerebellum, GABAergic. (Gad2$^+$) and glutamatergic vGluT2$^+$) neurons were targeted. In the cerebrum, general GABAergic and glutamatergic neuron populations were targeted, as well as mostly mutually exclusive GABAergic subpopulations expressing parvalbumin (PV) and somatostatin (SST).

PV$^+$ and SST$^+$ interneurons in neurodegenerative disease

We chose this experimental setup, as SST and PV neurons show differential responses in several neurodegenerative diseases and are expressed by two largely mutually exclusive* and morphologically and functionally distinct subpopulations[97,101,102].

In the broadest terms, PV$^+$ interneurons tend to be fast-spiking i.e, have higher firing frequencies with low input resistance and brief action potentials. They mainly target the soma, axon initial segment, or proximal dendrites of pyramidal cells or other interneurons. In contrast, SST$^+$ neurons predominantly target dendrites, have higher input resistance, low firing frequency, and longer sustained action potentials compared to PV$^+$ neurons (for a detailed review see[95]). These differences translate into distinct functional roles, with PV$^+$ neurons regulating the spiking output of pyramidal neurons of the cortex and hippocampus whereas SST$^+$ neurons control the excitability and integration of glutamatergic input to pyramidal neurons and control synaptic plasticity. SST$^+$ interneurons therefore also act as an important modulator of long-term potentiation in hippocampal pyramidal neurons[96].

The selective vulnerability of SST$^+$ and PV$^+$ neurons has been observed in several neurodegenerative diseases. In Alzheimer's disease models, SST$^+$ interneurons of the cortex and hippocampus exhibit selective vulnerability[103–105], which has been linked to deficits in

*While the majority of interneurons express either PV or SST, it should be noted that minor populations of neurons co-expressing PV and SST have been reported e.g. in the presubiculum.[101]

memory, executive function, and cognitive flexibility[104,106]. In contrast, hippocampal PV^+ neurons not only show higher resistance to disease but even compensate for the loss-of-function of SST^+ neurons by increasing their dendritic spine density[104]. In HD, PV^+ interneurons of the cortex and striatum are selectively vulnerable in patients and mouse models of HD[100,107], whereas SST^+ neurons appear mostly spared[100]. However, there is some evidence that aberrant activity of SST^+ neurons may also contribute to the increased GABAergic firing in HD[108].

A comparative study analyzing the loss of PV^+ neurons in FFI in contrast to gCJD and other prion diseases showed PV^+ neurons are comparatively well preserved in FFI. Moderate loss of PV^+ interneurons and neuropil occurs in the frontal cortex, while PV^+ neurons of the temporal and entorhinal cortex, pre- and parasubiculum, hippocampus, and cerebellum are well preserved and show normal morphology.[109] In contrast, gCJD (E200K) cases display pronounced loss of PV^+ neurons in all cerebral regions[109] parallel to a variable degree of spongiosis across regions[110]

Overall, these findings highlight the importance of investigating the distinct functional roles of various subpopulations of GABAergic neurons and their contribution to the pathogenesis of different NDs, and to further explore their differential vulnerability and the underlying mechanisms. The central role of PV^+ and SST^+ neurons in several NDs has made them a potentially interesting therapeutic target and we therefore decided to study these two cell types in more depth.

Considerations on Material and Methods

Papers I – III

Background on mouse models

In papers I-III, we studied mouse models of monogenic neurodegenerative diseases Creutzfeldt-Jakob disease (gCJD), fatal familial insomnia (FFI), and Huntington's disease (HD). In all three cases, we used knock-in models which express the disease mutation within the context of the mouse gene and at endogenous levels. We were interested in analyzing gene expression changes prior to the overt onset of clinical symptoms. Therefore, our translatome analysis was conducted at 9 months of age in all three models, which we found corresponded to a pre-symptomatic disease stage in all three models. Choosing the same time point in all models had the additional advantage that age-related changes would be comparable between models.

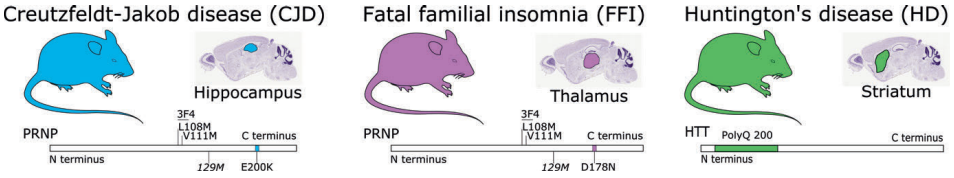

Figure 2: We analyzed knock-in mouse models for three genetic neurodegenerative diseases. Mice modeling genetic Creutzfeldt-Jakob disease carried the common E200K mutation in combination with the 129M polymorphism in the endogenous *Prnp* gene. In this model, the primary region affected by pathology is the hippocampus. Mice modeling fatal familial insomnia carried the D129N substitution in combination with the 129M polymorphism and show pathology in the thalamus, beginning at 12 months. Both prion disease models further carried the 3F4 epitope (L108M, V111M). In the Huntington's disease model, the CAG repeat stretch in exon 1 of the endogenous *Htt* gene was expanded to approximately 200 repeats.

Models for prion diseases

In paper I, we use knock-in mice carrying the mouse equivalent of the PRNP mutations found in human FFI (D178N-129M; Fig. 2) and gCJD (E200K-129M; Fig. 2), respectively[†]. These lines were previously characterized and found to replicate several key features of human diseases. FFI mice showed reactive gliosis in the thalamus at 12 months and the cerebellum at 16 months, followed by pronounced neuronal loss in the thalamus at 18 months[111]. In contrast gCJD mice developed spongiosis and aggregates of proteinase K-resistant PrP, especially in the hippocampus, emerging at 12-16 months of age[112]. Previously performed behavioral assessments revealed changes in both models beginning at 16 months[111,112]. This led to the overall conclusion that the 9 months' time point constitutes a pre-symptomatic disease stage in both disease models.

[†] Due to a single codon deletion at the N-terminus of the mouse *Prnp* gene, the mouse-equivalent mutations are located at codons 177 and 199, respectively. As per convention, we here use the human nomenclature also when referring to the respective disease-associated mutations in mouse models.

Huntington's disease model

In paper II, we used heterozygous knock-in mice carrying a pure CAG repeat stretch of approximately 200 repeats[‡] (Fig. 2). This line was originally maintained in a C57Bl/6 background[113,114], but around 20% of C57Bl/6 mice display nocturnal hyperactivity[115] that may exacerbate gene expression noise. Therefore, the HdhQ200 allele was backcrossed into the calmer 129S4 background, as was done for the FFI and CJD models (additional details can be found in the supplementary material of paper II). A detailed behavioral and neuropathological characterization of the 129S4-HD model was performed in paper II.

Cell type-specific expression of RiboTag

First published in 2009, the RiboTag[116,117] method uses the Cre-loxP system[118] to facilitate isolation of ribosome-associated mRNA by immunoprecipitation (IP) from cell types of interest within a complex tissue sample. RiboTag mice carry a loxP-flanked wild-type terminal exon of the large ribosomal subunit protein Rpl22, followed by a copy of the terminal exon expanded by three hemagglutinin-(HA)-tags. Crossing of Rpl22-HA mice with a Cre-driver line thus facilitates recombination between the two loxP sites, resulting in the excision of the wild-type exon and expression of the tagged exon in the targeted cell type. Rpl22-HA is subsequently integrated into the large ribosomal subunit where it is located on the surface of the protein complex, thus enabling immunoprecipitation with anti-HA antibodies (Figure 3). To activate the expression of the RiboTag transgene in our cell types of interest (Figure 1), homozygous RiboTag mice were crossed with homozygous Cre-driver mice.

For paper I, mice homozygous for mutated or wild-type *Prnp* and the RiboTag allele (gCJD: Rpl22-HA$^{fl/fl}$/Prnp$^{E200K/E200K}$, FFI: Rpl22-HA$^{fl/fl}$/Prnp$^{D178N/D178N}$, Control: Rpl22-HA$^{fl/fl}$/Prnp$^{wt/wt}$) were crossed to mice double homozygous for Cre and the respective *Prnp* allele. This made the breeding more efficient and economical, as all offspring could be expected to be heterozygous for Cre and the RiboTag transgene, and using a separate control group instead of littermates allowed us to use one set of control animals, reducing the overall number of animals required. A downside to this strategy was that the mice in our control group do not carry the 3F4 epitope which was added to create a transmission barrier in the prion disease mice. Creating a 3F4-control group would have required breeding additional five RiboTag and Cre-driver lines, the cost of which, regarding cage space and money, was prohibitive.

In paper II, Hdh$^{Q7/Q200}$/Rpl22-HA$^{fl/fl}$ mice were crossed with Hdh$^{Q7/Q7}$ mice homozygous for Cre. This resulted in offspring heterozygous for both Cre and RiboTag, with an expected 50% of offspring heterozygous for the HdhQ200 allele. This crossing scheme had the advantage of allowing us to use littermates as control animals.

[‡] The CAG repeat length was determined from ear clipping by fragment analysis. However, due to somatic expansion this is to be seen as an approximation.

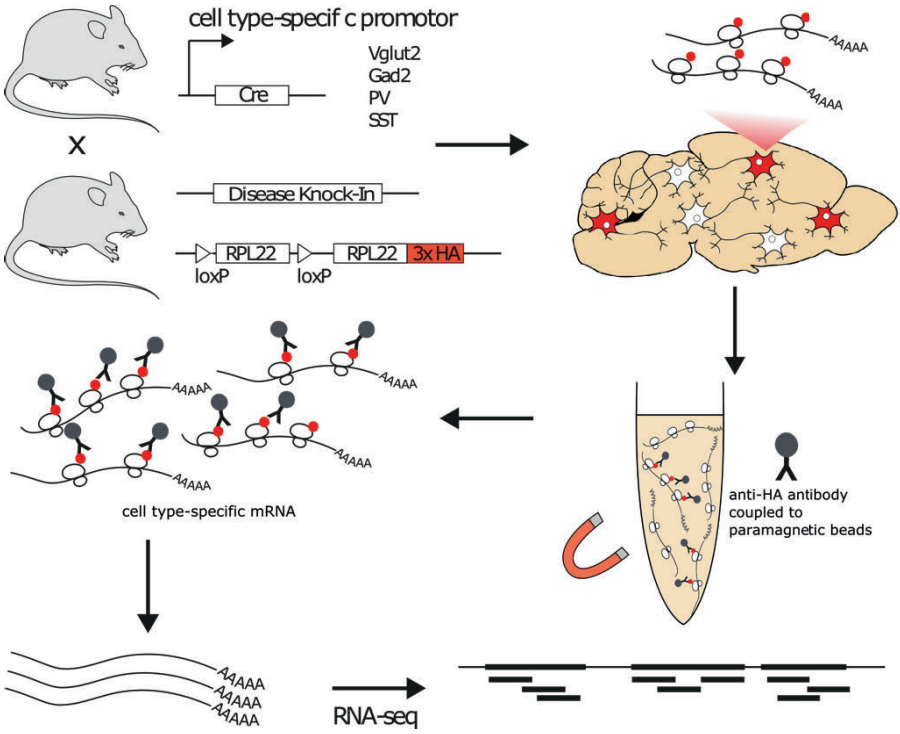

Figure 3: Basic RiboTag workflow. The RiboTag transgene consists of a floxed terminal exon of the large ribosomal protein gene 22 followed by a copy of the terminal exon expanded by a triplicated HA tag. To obtain experimental mice, animals carrying the mutated (or wild-type) disease gene and the sequence were crossed with Cre-Driver mice to activate expression of the RiboTag in the cell type of interest. Flash-frozen cerebral or cerebellar hemispheres were homogenized and tagged ribosomes immunoprecipitated using magnetic beads coupled with anti-HA antibodies, thus enriching polysomes and bound mRNA from the targeted cell type. Translating mRNAs are eluted and following quality assessment used to prepare sequencing libraries and sequenced.

RiboTag Immunoprecipitation

RNA sequencing analysis of bulk tissue results in the capture of total RNA, including pre-mRNA or RNA that is not translated, such as small or long non-coding RNA. In contrast, the RiboTag approach favors the extraction of translating mRNA, and the obtained samples are therefore more representative of proteins being created in the cell at the time of lysis. Here, we also refer to RNA samples obtained with RiboTag as “translatome” to highlight this difference in sample composition and to differentiate between RiboTag and total RNA samples.

RiboTag vs other methods for cell type-specific gene expression analysis

Several methods designed for cell type-specific analysis of gene expression exist, including other ribosome-tagging methods such as the bacTRAP technique[119], which uses a bacterial artificial chromosome (BAC) containing an EGFP-RPL10a fusion protein inserted into the

coding region of a marker gene[119] specific to the cell type of interest. The isolation of EGFP-tagged ribosomes and translating mRNA is conceptually identical to RiboTag. A disadvantage of bacTRAP is, that for each cell type of interest, a new transgenic mouse line must be generated, while RiboTag mice can be bred to pre-existing and validated Cre lines to obtain cell type-specific expression. Another advantage of RiboTag is that the transgene is expressed from the endogenous Rpl22 locus, whereas with bacTRAP the expression is driven by the marker gene,[119] and therefore creates a surplus of tagged ribosomal protein competing for integration into polysomes[120]. In contrast, a disadvantage of RiboTag is that two transgenes are needed, usually resulting in a more complicated breeding scheme, whereas bacTRAP requires only one.

A very different approach is single-cell RNA sequencing (scRNAseq) which is a high-throughput method for studying gene expression at a cellular level. For this, cells are physically separated, for example by encapsulating single cells into nanoliter-sized droplets using a microfluidic system[121]. RNA molecules from individual cells are then isolated, tagged, and sequenced. This makes scRNAseq a powerful method to analyze heterogeneity within a given population of cells, for *de novo* identification of rare cell types, and to study responses or disease states in different cell types. scRNAseq has the advantage that it does not require the time-consuming and expensive creation of a transgenic model and can therefore also be used to analyze human samples. It also better divides cell types with similar properties than RiboTag and bacTRAP. However, a considerable disadvantage of scRNAseq is its limited capture efficiency. Drop-out events -the failure to detect an expressed gene- are frequent, and variability in gene dropouts between cells can erroneously be interpreted as biological differences. While this issue is avoided with RiboTag, a disadvantage of RiboTag is that the targeted cell population is defined by the precision of the Cre-driver line, making it impossible to determine whether the expression of a specific gene varies between subpopulations.

Workflow and protocol adjustments for RiboTag samples in papers I and II

In papers I and II, flash-frozen brain samples were homogenized in polysome buffer, which contains a mix of cycloheximide, protease and RNase inhibitors to halt translating ribosomes and prevent RNA degradation. Before the isolation of polysome-bound mRNA, 200 µl of homogenate was aliquoted to isolate total RNA, which was used as a comparator to confirm enrichment of cell type-specific mRNA by RiboTag. To minimize the capture of unspecific mRNAs bound to antibodies or beads, the pre-clearing step was modified in the RiboTag IP workflow. For this, the homogenate was incubated with beads bound by isotype-control antibodies (IgG). The pre-cleared homogenate was then incubated with an anti-HA antibody to capture tagged ribosomes, which were then bound to ProteinG-labeled paramagnetic dynabeads (Figure 3). Following washing steps in buffers with increasing salt concentrations, ribosome-bound mRNA was extracted and purified using Qiagen RNeasy spin columns.

For samples from prion-diseased mice and respective controls used in paper I, we needed to inactivate any potential remaining infectious protein. While our protocol for RNA preparation made it highly unlikely that any protein remained in the samples, this was necessary to

sequence the samples outside of a Bio Safety Level 3 environment. We, therefore, introduced an additional incubation step with the chaotropic agent guanidine isothiocyanate (GdnSCN). Even at room temperature, incubation of homogenized CJD brain tissue with 4 M GdnSCN for 25 min has been shown to reduce the titer by around 5 logs[122]. Additionally, GdnSCN is a common ingredient lysis buffer and is routinely used to inactivate RNase or DNAses during nucleic acid isolation, thus making it a good option to reduce any potentially remaining infectivity without impacting RNA quality.

Library preparations and RNAseq

A cell's total RNA is typically made up of 80-90% ribosomal RNA (rRNA), whereas mRNA makes up only around 5-10%. While RiboTag results in the depletion of several non-coding RNA species such as miRNA, lncRNA, or snoRNAs, samples still contain a high percentage of rRNA. As these would create noise and take up valuable sequencing capacity, reducing read depth for mRNA reads, mRNA enrichment by oligo-d(T)-beads was performed for all samples prior to library preparation. Libraries for both RiboTag and total RNA were generated using the Illumina TruSeq Stranded mRNA kit.

Library preparations and sequencing were performed at the National Genomic Infrastructure (NGI), Uppsala. Samples prepared for papers I and II were processed and sequenced together, to allow for comparability between the different diseases. All samples were sequenced on an Illumina S4 flow cell, which has four physically separated sequencing lanes. To minimize batch effects, replicates from each group were randomly split across the lanes. The raw sequencing data have been deposited in the Gene Expression Omnibus (GEO) repository where they are available under accession numbers GSE198063 (FFI and gCJD) and GSE199837 (HD).

Preprocessing and quantification of sequencing reads

Transcript quantification was performed using the nf-core/rnaseq pipeline[123,124]. This Nextflow-based bioinformatics pipeline provides a reproducible analysis workflow to quantify gene expression from raw FASTQ files. Besides alignment and quantification, this workflow includes quality control and pre- and post-processing steps and allows the user to choose between several common aligners, reference genomes, and processing tools. The pipeline codes are available as tagged stable versions on GitHub, thus offering full reproducibility.

All samples were processed with the nf-core/rnaseq pipeline version 3.0. Prior to alignment, quality control was performed with fastQC and sequencing adapters and low-quality bases were trimmed with TrimGalore. To quantify transcript expression from reads, we used the pseudo-alignment tool salmon[125]. In contrast to traditional alignment tools, which align reads to the reference genome in a time and resource-intensive step, salmon presents a combined pseudo-alignment and quantification tool. Salmon creates an index file of the transcriptome and their corresponding position to which the reads are mapped. From this, the abundance of each transcript is calculated. As a result, salmon is considerably faster and less resource intensive.

Differential gene expression analysis

In papers I-III we used DESeq2[126] to identify statistically significant differences in expression levels between conditions. To reduce the number of genes that would likely be uninformative we removed genes with low expression and non-protein coding genes by prefiltering.

To account for differences in library size and RNA composition between samples, normalization of raw counts is performed by dividing them by a sample-specific size factor. The size factor is calculated using the row-wise geometric mean across all samples, creating a pseudo-reference sample. For each sample, the ratio of each gene to the reference is calculated median sample ratio is set as a sample-specific size factor used to normalize gene counts. As samples are compared on a gene level, normalization to gene length was not required.

Gene set analysis

Following analysis with DEseq2, we next analyzed the enrichment of biological pathways or processes. Here, we used two common approaches to conduct functional analysis: overrepresentation analysis (ORA) and gene set enrichment analysis (GSEA). The former method uses a list of selected genes as input and tests whether these are significantly overrepresented among genes in an annotated gene set. This is useful as it can efficiently summarize genes into shorter lists of pathways or processes. In contrast, GSEA considers the expression levels of all genes detected in a sample.

Gene set libraries

A gene set constitutes a group of genes with a known association e.g., involvement in a biological pathway, cellular compartment, or disease, which are compiled into a collection referred to as gene set libraries. While sets may be based upon interacting gene products, the gene sets do not convey hierarchical information.

The following gene set libraries were used in papers I-III:

KEGG pathways: Includes a collection of gene products involved in a given biological process based upon the collection of pathway maps maintained by the Kyoto Encyclopedia of Genes and Genomes (KEGG)[127,128].

Gene Ontology libraries: The Gene Ontoloy (GO) project[129] is a continuously updated database of available functional knowledge on genes in the form of annotations with a controlled vocabulary. The ontology terms are organized into three broader domains representing different aspects of gene function.

- **Cellular component (CC)**: describing the parts of a cell associated with a gene product.
- **Biological processes (BP)**: larger scale cellular mechanisms or systems associated with a gene product (e.g., “translation”, “cell division”).
- **Molecular function (MF)**: molecular activity of a gene product (e.g., “oxidase”).

GO terms are organized in a loose hierarchical structure, with more specialized “child” terms summarized under broader “parent” terms[130]. This often results in redundancy as results are

likely to contain highly similar, related terms. To reduce this, methods have been developed to summarize terms based on their semantic similarity[131]. However, since a child term can belong to several parent terms, this process can yield ambiguous results.

ChEA: The ChIP Enrichment Analysis (ChEA) application integrated into the Enrichr package[132], provides an analytical tool to test for overrepresentation of mammalian transcription factor targets as determined by various chromatin immunoprecipitation methods (ChIPseq, ChIP-chip, ChIP-PET, DamID). As such, it can be used as a tool to link gene expression changes to transcription factor binding sites[133].

Overrepresentation analysis

In papers I-III, the Enrichr[132] R package was used in several instances to conduct ORA on a defined subset of genes, e.g. DEGs or module gene lists. This method uses Fisher's exact test to determine the significance of enrichment i.e., the probability of observing an equal or more extreme enrichment of input genes by chance. This approach assumes a binomial distribution and independence for the probability of gene set membership of an input gene. As gene set libraries usually contain several hundred gene sets, multiple testing correction (here: Benjamini-Hochberg) is performed. The Fisher exact test is biased towards gene set size, with larger gene sets tending to have lower p-values. To mitigate this, Enricher also calculates a rank or z-score, as well as a proprietary combined score for each gene set[132], which was used in papers I-III. The z-score indicates the deviation of a presumed enriched gene set from the expected rank. To this end, a "background" is calculated for each gene set library, using random input genes to calculate an expected average rank for a gene set of any given size and provides a z-score that indicates the deviation of a presumed enriched gene set from the expected rank. The combined score is calculated by multiplying the log-transformed p-value for a gene set with this z-score ($c = \ln(p) * z$).

Gene set enrichment analysis

ORA is useful to detect unifying functional associations among a predefined selection of genes e.g., DEGs. However, the selection of DEGs is based on a usually arbitrary significance cut-off, which introduces bias by excluding genes with more modest expression changes. Still, changes in a group of genes involved in the same pathway may be relevant to the disease phenotype, even if none of the genes fulfill the criteria of differential expression. To address some of these shortcomings, we performed gene set enrichment analysis (GSEA)[134,135]. This also allowed us to gain an understanding of altered pathways or processes in cell types for which only a few DEGs were detected, and for which we therefore could not obtain reliable results with ORA.

Rather than testing enrichment in a predefined subset of genes, GSEA assesses the correlation of gene sets with the phenotype using a ranked list of all genes as input, allowing for a more comprehensive analysis. A variety of gene-level statistics can be used for ranking, but commonly a score is calculated by multiplying the sign of the fold change by -log10(p-value)

so that the rank reflects both significance and direction of change, with the most upregulated DEGs located at the top of the list and downregulated at the bottom of the list[134]. The association with the phenotype is assessed for each member of a gene set by analyzing the distribution of genes in the rank list. Gene set statistics are then calculated by combining the gene level statistics for a given set and assessing the significance of association with the phenotype by repeated randomization of genes (referred to as "gene sampling").
Different statistical methods for calculating gene set significance and randomization are in use, with little agreement on a standard[136], leading to varying results between different analyses. To address this issue, we used the piano R package[137], which offers a range of statistical methods with the option to combine results into a consensus score.
Additionally, the piano package provides p-values for different directionality classes (non-, mixed-, or distinct directional). In the non-directional class, gene-level statistics on the directionality of change are not considered during analysis, therefore a significant gene set in this class can be interpreted as being affected by differential expression in general. For distinct directional classes, two runs are performed, testing for up- and downregulated gene sets. Thus, this approach detects gene sets that are significantly affected by differential expression in one direction. Gene sets significantly affected in both directions will not be considered with this method. This use of directionality classes is a useful addition to traditional GSEA, introducing a statistical measure to determine whether processes or pathways are altered in a specific direction. However, interpreting the biological significance of this information is more complex since GSEA identifies sets of functionally related genes, but without considering the underlying regulatory processes, gene functions, and interactions.

General workflow for GSEA with piano

1) Genes were ranked by gene-level statistics (p-value and log fold change) obtained from DESeq2.

2) Six different statistical methods were used to calculate gene set statistics. We analyzed enrichment for the KEGG pathway and GO Biological Process libraries in different directionality classes, analyzing each cell type in each disease separately. Multiple testing correction was performed using the Benjamini-Hochberg method.

3) Consensus Scoring: To consolidate results from the different GSEA analyses, a consensus score is calculated based on ranking gene set p-values from the same directionality class obtained from the different methods. The mean minimal rank for each gene set is used as the consensus score.

Network Analysis

Gene co-expression networks are used to identify clusters of genes with similar expression patterns across experimental conditions, based on the assumption that genes that share expression patterns are functionally associated -due to being part of the same complex or pathway and therefore being affected by the same regulatory mechanisms, or due to influencing

each other directly or indirectly. Analyzing the properties of a gene co-expression network can thus be used as a hypothesis-building tool that can help explore novel putative gene functions and pathways[138,139].
Highly correlated genes form dense clusters or modules within a network, which can then be correlated with a phenotype[139]. Graph theory can be applied to analyze the topological properties of a network, i.e., the arrangement of nodes (here representing genes) within a network. This can be used to identify central nodes within a network substructure by applying different measures of centrality. One of the simplest measures which we applied in paper I is the degree centrality of a node, which described the number of links (connections) of a given node. This was used to identify highly interconnected genes, also referred to as "hub" genes. The identification of central genes is useful based on the assumption that these genes are likely to have a central role within functional clusters. Consequently, one can hypothesize that if central genes were to be affected in a disease context, this may have far-reaching biological consequences and that these genes may therefore be of interest as therapeutic targets[140].

Construction of a weighted gene co-expression network for SST samples

In paper I, we performed analysis on a weighted, undirected gene co-expression network of SST^+ samples. After filtering out lowly expressed genes, we used Spearman's rho to compute the pairwise correlation of genes across samples, based on normalized expression values (TPM). Correlations with FDR < 0.01 and Spearman rho > 0.82 were considered when constructing the weighted network, where rho was used as edge weight.
Modules were detected using the Leiden algorithm[141], which identifies densely interconnected clusters based on their modularity. Modularity quantifies the division of a network into distinct communities of nodes by calculating the difference between the number of edges within communities and the expected number of edges within communities in a random network. Thus, a modularity value close to 1 indicates a network with well-defined communities where nodes are more densely connected within their given community than with nodes outside their community. The Leiden algorithm starts by treating each node as its own cluster, and then iteratively merging clusters in a way that maximizes the modularity function. In contrast to the earlier developed Louvain algorithm, the Leiden method avoids sub-optimal clustering by allowing a refinement step, in which a node is moved to neighboring clusters to maximize modularity within each cluster (local refinement) or two clusters are merged (global).

It should be noted that this approach differs slightly from the WGCNA algorithm as developed by Horvath and Langfelder[139]. While the core principles are the same, the WGNCA approach allows soft thresholding which is used to raise the value of correlation to enhance the detection of weaker co-expression patterns. However, this can also lead to the addition of spurious edges, especially in a network based on comparatively few samples, as is the case in paper I.

RNA In-situ hybridization

In paper II, we used RNAscope to validate the observed changes in *Ccnd1* mRNA expression in formalin-fixed, paraffin-embedded (FFPE) brain tissue sections of 9-month-old S4-

HdhQ200 and control mice. RNAscope[142] relies on the use of probe pairs that bind to adjacent 18 to 25 bp sequences in the target gene. This increases the specificity of detection and reduces background noise as the binding of both probes is required for successful detection by a pre-amplifier probe. The combination of up to 20 such probe pairs results in a well-labeled target RNA. In subsequent steps, sequential rounds of hybridization with amplifier and pre-amplifier molecules are performed to enhance the signal, making it possible to detect even single mRNA molecules as puncta. In paper II, FastRed was used for labeling as this allowed detection by both brightfield and fluorescent microscopy. In addition to validating the differences in gene expression which we detected in our RNAseq data, this approach also provided spatial information, allowing us to observe changes in mRNA expression in the histological context.

Imaging and Quantification

For ISH of *Htt* mRNA, we counted individual puncta per cell (Paper II) for quantification. However, the high expression of *Ccnd1* and the densely packed morphology of the granular layer made it challenging to apply the same approach for staining of *Ccnd1* mRNA. Therefore, we opted to quantify the staining by comparing the intensity in the granular layer between HD and control samples. To this end, stained sections were imaged by laser confocal microscopy to obtain z-stacks of optical sections throughout the entire thickness of the tissue section (4 µm). Brain hemispheres for age-matched disease and control animals were embedded in the same cassette to ensure consistent treatment of sections and reliable quantification, thus ensuring consistent staining and imaging conditions between disease and control samples.

Paper IV

Molecular cloning

For the generation of plasmids in paper IV, we primarily used two molecular cloning methods: conventional restriction enzyme digest followed by ligation, and Gibson assembly (using the HiFi DNA Assembly protocol by NEB), which allows ligation of multiple DNA fragments in a single reaction using overhangs between adjacent fragments.

CRISPR-guided homologous recombination

The transgenes were incorporated into the genomic DNA by homologous recombination, a conserved cellular mechanism to repair double-strand breaks (DSBs) in DNA, usually using the intact chromosome as a template. A donor plasmid containing the transgene flanked by homology regions can act as an alternative template when introduced into the cell. To make the integration more efficient, we used the bacterial CRISPR-Cas9 to introduce targeted DSBs. For each locus, we designed two guide RNAs (gRNA) to guide the Cas9 nuclease to the target sequence where it introduced a DSB either inside the 3'UTR or downstream of the 3'UTR.

ESC culture

Donor plasmids were transfected into J1 mouse embryonic stem cells (SCRC-1010, ATCC). These cells were re-cloned from J1 ESCs derived from a male 129/SvJae embryo[143]. This cell line was used as the eventual goal of this project was to generate a new Tagger mouse line, which was previously done in 129S4 mice. ESCs were cultured on a feeder monolayer of DR4 mouse embryonic fibroblasts. Feeders were irradiated to prevent proliferation and carry multi-drug resistance against several antibiotics, including neomycin/geneticin.

Aims

The general aim of this thesis was to analyze cell type-specific gene expression changes in three models of neurodegenerative disease in an early, pre-symptomatic disease stage.

Paper I

Using RiboTag, we wanted to compare cell type-specific gene expression responses of six cell type in mouse models of genetic Creutzfeldt-Jakob disease and fatal familial insomnia at a pre-symptomatic disease stage.

Paper II

Characterization of the HdhQ200 knock-in mouse model in a 129S4 background and cell type-specific translatome changes in pre-symptomatic Huntington's disease.

Paper III

Systematic comparison of gene expression changes in Parvalbumin-expressing neurons in Creutzfeldt-Jakob disease, Fatal familial insomnia, and Huntington's disease models.

Paper IV

Generation of targeting vectors for three potential genomic safe harbor loci, comparing two transgene expression systems on integration efficiency and their effect on endogenous gene expression.

Results and Discussions

Paper I

Translatome profiling in fatal familial insomnia implicates TOR signaling in somatostatin neurons

In paper I, we investigated cell type-specific translatome changes in mouse models of gCJD (E200K) and FFI (D178N) using RiboTag. We analyzed six cell types (vGluT2$^+$ and Gad2$^+$ neurons in the cerebrum and cerebellum, and cerebral PV$^+$ and SST$^+$ neurons) in both disease models and age-matched controls, with 3-7 replicates in each group.

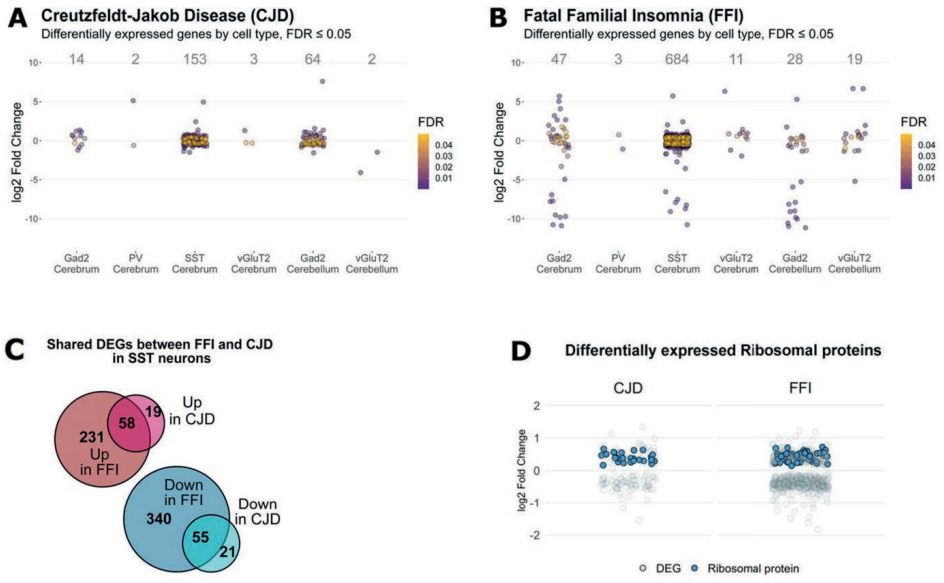

Figure 4: (A, B) Differentially gene expression analysis of targeted cell types in CJD (A) and FFI (B). (C) The majority of DEGs detected in CJD were also detected in FFI, suggesting a similar response between the diseases (D) Both CJD and FFI display a mild but concertized up-regulation of ribosomal protein genes in somatostatin-expressing neurons with 26 of 79 ribosomal proteins significantly up-regulated (FDR ≤ 0.05) in CJD and 57 in FFI.

We first performed differential gene expression analysis for each cell type in both diseases (Fig. 4 A, B). Since PV$^+$ neurons were previously reported as early vulnerable, we expected to see a comparatively strong response in form of high numbers of DEGs in this cell type. We also expected to see pronounced changes in cerebral vGluT2$^+$ neurons, since this constitutes the cell type in the most affected brain regions in both CJD (hippocampus) and FFI (thalamus) and expressed the highest levels of *Prnp*. However, we found only few DEGs in either cell

type. A possible explanation is that expression changes from the affected brain regions were not detected as they constitute only a subset of targeted neurons in cerebral vGluT2^{+} samples and may therefore have been "diluted". For PV^{+} neurons, GSEA showed enrichment of gene sets associated with neuronal dysfunction. We further observed a considerably stronger response in a later study (paper III), that indicated our analysis may have been underpowered.

Surprisingly, we observed the strongest response in SST^{+} neurons, with 684 DEGs in FFI and 153 DEGs in CJD. The majority (74%) of genes seen in CJD were also detected in FFI (Fig. 4 C), indicating a similar response in both diseases, including a mild (average LFC = 0.42 in FFI; 0.44 in CJD) but coordinated upregulation of ribosomal protein genes (Fig. 4 D). Functional analysis corroborated these results, indicating changes in several shared pathways including upregulation of translation, and downregulation of genes associated with axon extension and synaptic organization.

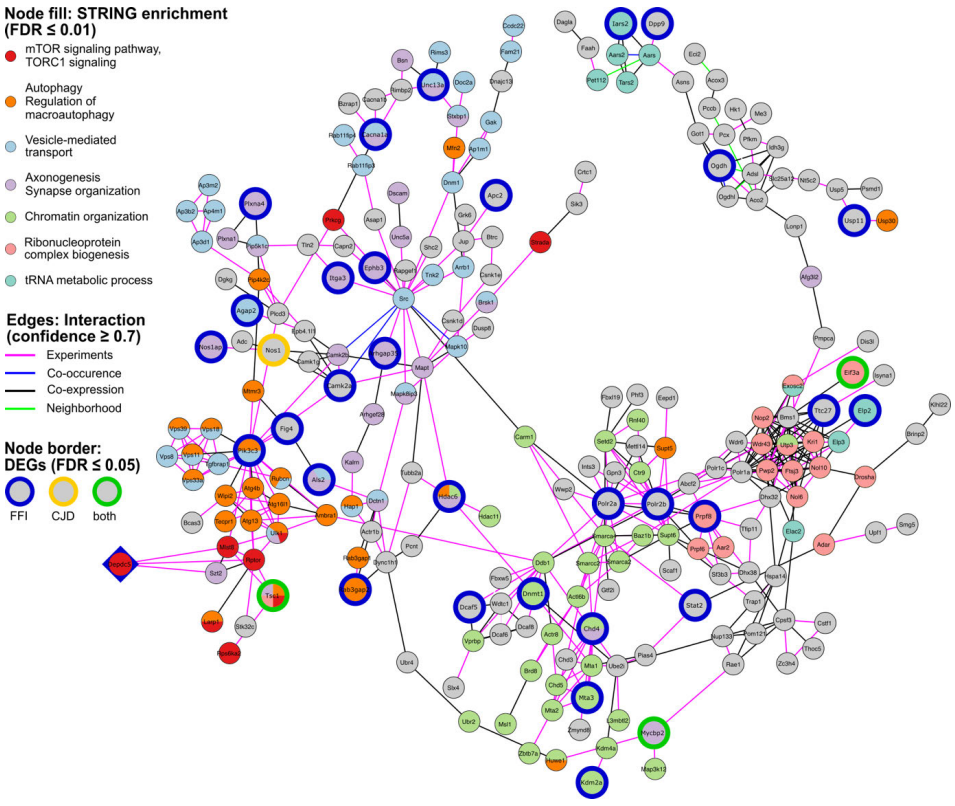

Figure 5: Largest connected component of a PPI network for module 1 hub gene *Depdc5* (diamond-shaped) and first-degree neighbors. Larger nodes with colored borders indicate DEGs by disease. Node colors show selected functional associations of genes based on STRINGdb enrichment (FDR ≤ 0.01).

Hippocampal SST^+ neurons are affected in early Alzheimer's disease[103,104,106], but we do not know of similar reports in PrDs, which prompted us to investigate this cell type more closely. To this end, we constructed a weighted gene co-expression network and identified six topological modules and their hub genes. Of the identified hub genes in module 1, three were also significantly downregulated in FFI: *Depdc5,* a subunit of the mTOR inhibitor complex GATOR1[144], *Mta3*, which encodes a subunit of the nucleosome remodeling and deacetylation complex (NuRD), which facilitates rRNA transcription by establishing a poised promoter state[145,146], and *Gtf3c1,* a component of the essential transcription factor TfcIIIC, required transcription of tRNAs and 5S RNA. We used the StringDB database to interrogate connections between these hub genes and their first-degree neighbors for evidence of protein-protein interactions (PPIs). Surprisingly, this yielded no results for *Gtf3c1*. PPI networks included approximately 40% of the identified neighbor genes (*Depdc5*: 230/560, *Mta3*: 220/551), which were further significantly associated with mTOR signaling, ribonucleoprotein complex biogenesis, regulation of autophagy, chromatin organization, and vesicle-mediated transport. Additionally, the mTORC1 inhibitor Tsc1 was also downregulated in both diseases (Fig. 5).

We observed concerted upregulation of ribosomal protein genes in SST^+ neurons and identified differentially expressed hub genes associated with mTOR inhibition and regulation of rRNA transcription. We therefore speculate whether altered mTOR activity underlies these changes, as mTOR is a central regulator of cellular metabolism, promoting anabolic processes such as protein synthesis and mitochondrial biogenesis and respiration, while negatively regulating catabolic processes like autophagy[147]. Additionally, mTORC1-regulation of ribosome biogenesis is suggested as a mechanism to control molecular crowding and phase separation[148], affecting internal biophysical properties and morphology of neurons. Activation of mTOR in neurons has been suggested to have both positive and negative effects on neuronal survival. For example, mTOR-dependent local translation in dendrites and axons is important in injury response[149] and long-term synaptic plasticity[150]. However, mTOR activation has also been associated with impaired autophagic clearance of protein aggregates[151]. Furthermore, there is also increasing evidence pointing towards ribosomal proteins having a multitude of, likely protein-specific, extra-ribosomal functions, including p53 activation and regulation of immune response[152]
In summary, given the complex and multifaceted roles of both ribosomal proteins and mTOR, further investigation is needed to validate and determine the relevance of the observed changes. Given that SST^+ neurons have not been known to be vulnerable in early prion disease, the question remains whether these are detrimental, or potential constitute an adaptive response.

This was the first study providing a comparative analysis of cell type-specific gene expression changes in pre-symptomatic genetic prion disease. In summary, our findings indicated that SST^+ neurons are affected in early the disease process, although further validation of these findings is needed. We also found both diseases show more similarities in differentially expressed genes and functional enrichment than expected given their differences in symptoms and pathology.

Paper II

Cerebellar granule neurons induce Cyclin D1 before the onset of motor symptoms in Huntington's disease mice

Reports on cerebellar pathology in HD predominantly describe the loss of Purkinje cells coupled with apparent resistance of cells in the granular layer[45,52,53]. Recently, increasing attention has been placed on the potential role of the cerebellum in the HD phenotype[51,153]. Analysis of gene expression changes in the cerebellum indicated that similar pathways are affected as in the striatum[47,49]. However, none focused on cell type-specific expression patterns.

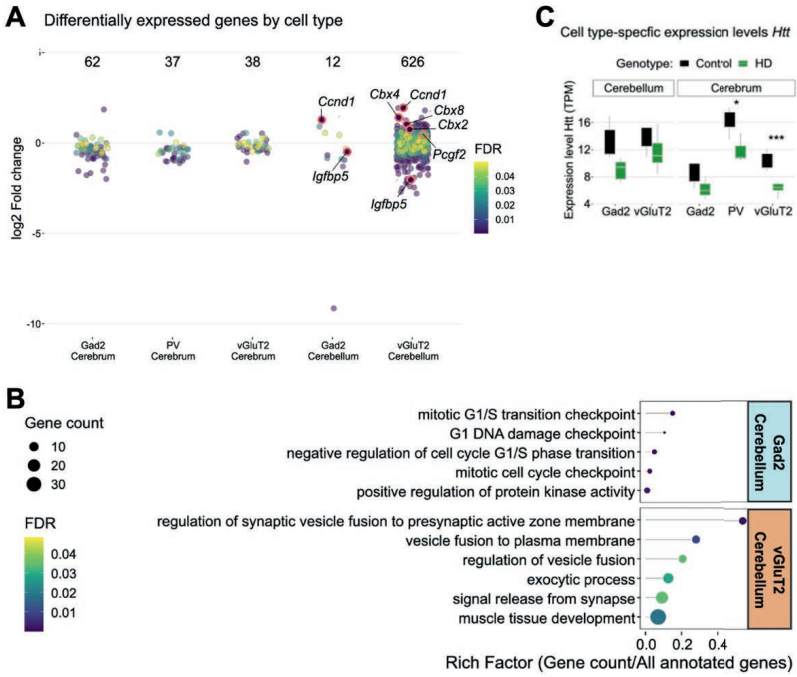

Figure 6: (A) Differentially expressed genes (DEGs) (FDR ≤ 0.05) for each cell type. (B) Top five significantly enriched terms (FDR ≤ 0.05) among DEGs reveal cell type-specific responses to mHtt. (C) Expression levels of Htt mRNA were slightly reduced in all cell types, significantly in cerebral vGluT2$^+$ and PV$^+$ neurons (* FDR ≤ 0.05; ** FDR ≤ 0.01; *** FDR ≤ 0.001).

Using RiboTag, we isolated translating mRNA from cerebral (vGluT2$^+$, Gad2$^+$, PV$^+$) and cerebellar (vGluT2$^+$ and Gad2$^+$) neurons, focusing on cerebellar cell types. To our surprise, we observed the strongest response with 626 DEGs in glutamatergic (vGluT2) neurons of the cerebellum, a population that predominantly consists of granular neurons -a cell type not usually reported as vulnerable in HD[45]. In contrast, we only found 12 DEGs in GABAergic

neurons, which includes Purkinje cells (Fig 6 A). Investigation of functional associations of these genes with ORA revealed enrichment of biological processes associated with neurotransmission, vesicle fusion, and exocytosis in vGluT2^{+} and cell cycle re-entry in Gad2^{+} neurons of the cerebellum (Fig. 6 B). We further found comparatively strong upregulation of cyclin D1 (*Ccnd1*) (LFC = 1.8 in vGluT2^{+} and 1.3 in Gad2^{+}). This was also confirmed by *in-situ* hybridization for *Ccnd1* mRNA, which showed a 1.8-fold increase in staining intensity in the granular layer (Fig. 7). Ccnd1 is a key regulator of G1/S transition and increased levels of Ccnd1 in normally post-mitotic neurons results in aberrant cell cycle reentry and has been linked to neurodegeneration by inducing apoptosis[154–157], or may cause cells to dedifferentiate[158–160].

GSEA indicated that both apoptosis and differentiation-related gene sets were significantly enriched in vGluT2^{+} neurons (Fig. 8), though we have not attempted to further validate this in the current study. We additionally observed upregulation of Cbx family protein gene (*Cbx2, Cbx4, Cbx8*) (Fig. 6 A), which form one of the core elements of canonical PRC1 and have been implicated in the regulation of cell cycle regulation and DNA damage response[161,162].

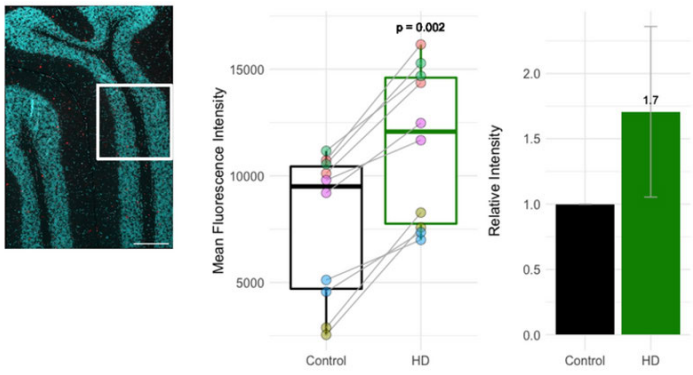

Figure 7: Quantification of mean fluorescence intensity in the granule layer of lobule IV/V (white square). Analysis was performed on two measures obtained from five biological replicated per group. At 9 months, HD samples (n = 10, Shapiro-Wilks: W = 0.87, p = 0.11) show a significant 1.7-fold increase of *Ccnd1* staining compared to controls (n = 10, Shapiro-Wilks test: W = 0.83, p = 0.03), Wilcoxon rank sum test, p = 0.002, n = 10, matched control and HD samples are indicated by dot color and connecting line

As this study also marked the first use of the HdhQ200 model in a 129S4 background, we performed behavioral and histopathological characterization of these mice. Behavioral assessment between 3 and 18 months using the accelerating rotarod, balance beam, and burrowing tasks[163] revealed only mild behavioral disturbances beginning at 12 months, consistent with the observations made in the C57Bl/6 background[113,114], and importantly, no hyperactivity. Taken together, these experiments confirm 9 months as a pre-symptomatic disease stage in the S4-HdhQ200 mouse model. Histopathological assessment was conducted by analyzing the presence and cellular location of proteinase K-resistant Htt^{+} aggregates. This revealed that HD mice showed disease-typical NIIs by 9 months, especially in the striatum,

hippocampus, and cerebellum. *In-situ* hybridization for *Htt* mRNA indicated a reduction of *Htt* levels in the cortex and hippocampus at 9 months. This was corroborated by RNAseq analysis revealing a significant reduction of *Htt* expression levels in cerebral PV^+ and $vGluT2^+$ neurons (Fig. 6 C), which is consistent with the predominant cell types in these brain regions.

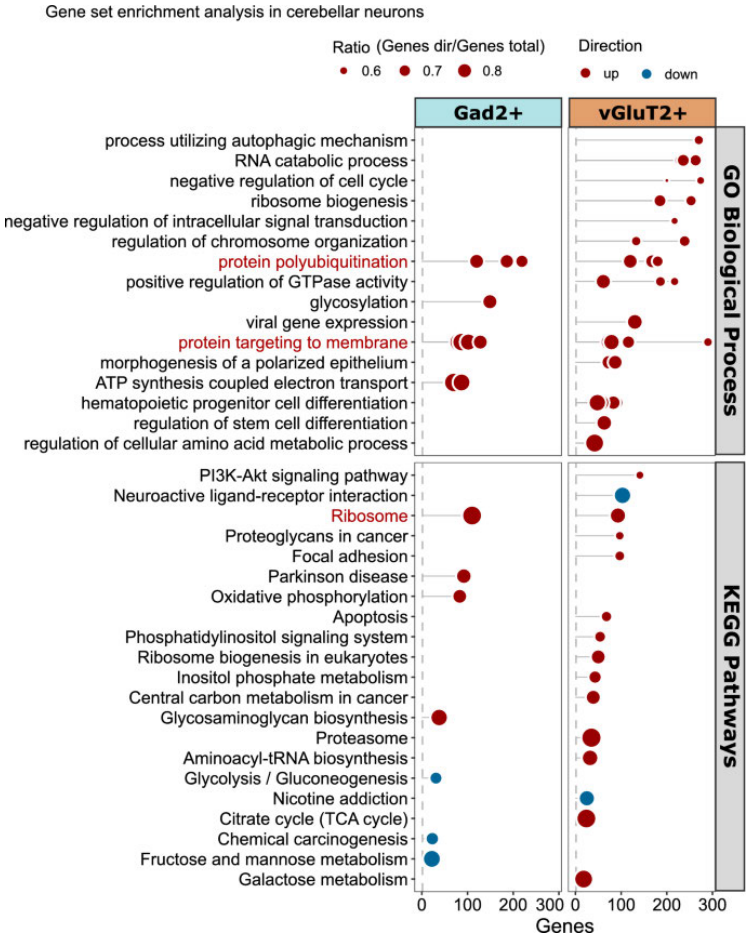

Figure 8: GSEA shows a mostly cell type-specific response in $Gad2^+$ and $vGluT2^+$ cerebellar neurons. $vGluT2^+$ neurons show enrichment of apoptosis pathway and differentiation-associated terms. Shared GO terms are indicated in red. Ratio indicates the relative number of enriched genes to gene set size.

In conclusion, Paper II provided novel insights into molecular and neuropathological changes in the cerebellum in pre-symptomatic HD. This study indicated that in particular glutamatergic neurons of the granular layer showed considerable gene expression changes prior to the onset of overt symptoms.

Paper III

Comparative analysis reveals disease-specific responses in parvalbumin-expressing neurons at early disease stages

PV^+ interneurons show early vulnerability in various neurodegenerative diseases, including HD[100,164], CJD[110,165], and FFI[109]. Cortical PV-INs show aberrant firing behavior in Huntington's disease, which may contribute to motor symptoms[100,166], and striatal PV^+ neurons, while not as vulnerable as striatal MSNs, are among the earlier lost cell types in HD[100,107]. Loss of cortical PV-INs and their perineuronal net has also been reported in CJD patients[165,167] and to a lesser extent in FFI[168], even in otherwise morphologically normal tissue. However, in our previous study (paper I), we did not observe pronounced gene expression changes although GSEA suggested ER protein processing, ribosome biogenesis, autophagy, and synapse organization are affected in PV^+ neurons (see paper I).

In paper III, we therefore conducted a comparative analysis of PV^+ translatome samples in all three disease models (gCJD, FFI, and HD), combining samples from the datasets generated for papers I and II. The processing of prion samples and their respective controls required minor adjustments to the RiboTag protocol to inactivate any potentially remaining infectious species. While we did not expect this to result in any obvious batch effect between the two control groups, we performed sample-wise correlation and principal component analysis, which confirmed that there were no obvious differences between groups.

Differential expression analysis was performed for each disease group, comparing against the combined controls. In contrast to results from paper I, in which we observed only 2 DEGs in gCJD and 3 DEGs in FFI, we now found 91 DEGs (FDR $\leq$ 0.01) in gCJD samples (Fig. 9), including seven ribosomal protein genes and translation elongation factors. Consequently, ORA indicated significant enrichment of terms associated with translation, but also the regulation of intracellular signal transduction, which notably included upregulated genes associated with cell cycle regulation and apoptosis such as *Bok* and *Nupr1*. The 52 DEGs identified in FFI were overrepresented among genes associated with synaptic assembly. Our earlier study on HD (paper II) indicated DEGs were predominantly associated with myelination and neurotransmitter reuptake, which we could not confirm here. Due to the low number of DEGs identified in PV samples, ORA was not attempted in paper I.

Seven genes were shared between PrDs, without any significant functional association, while there was no overlap with HD. This may be due to the low number of DEGs in HD, but could also indicate that gCJD and FFI show an overall more similar response than HD. To further investigate disease-specific responses, we next performed gene set enrichment analysis using the same approach as applied in papers I and II. This revealed several differences between diseases. In gCJD we observed upregulation of inflammation-associated pathways, which is consistent with both, our earlier findings (paper I) and reports on sporadic CJD[86,169]. Notably, the same pathways were downregulated in HD, which we did not detect in our earlier analysis

but is in keeping with the absence of gliosis in this model (paper II). HD neurons showed changes in a variety of pathways including upregulation of autophagy, downregulation of developmental programs and aberrant methylation. Strikingly, we also observed the downregulation of circadian entrainment and upregulation of ND pathways not previously observed in FFI.

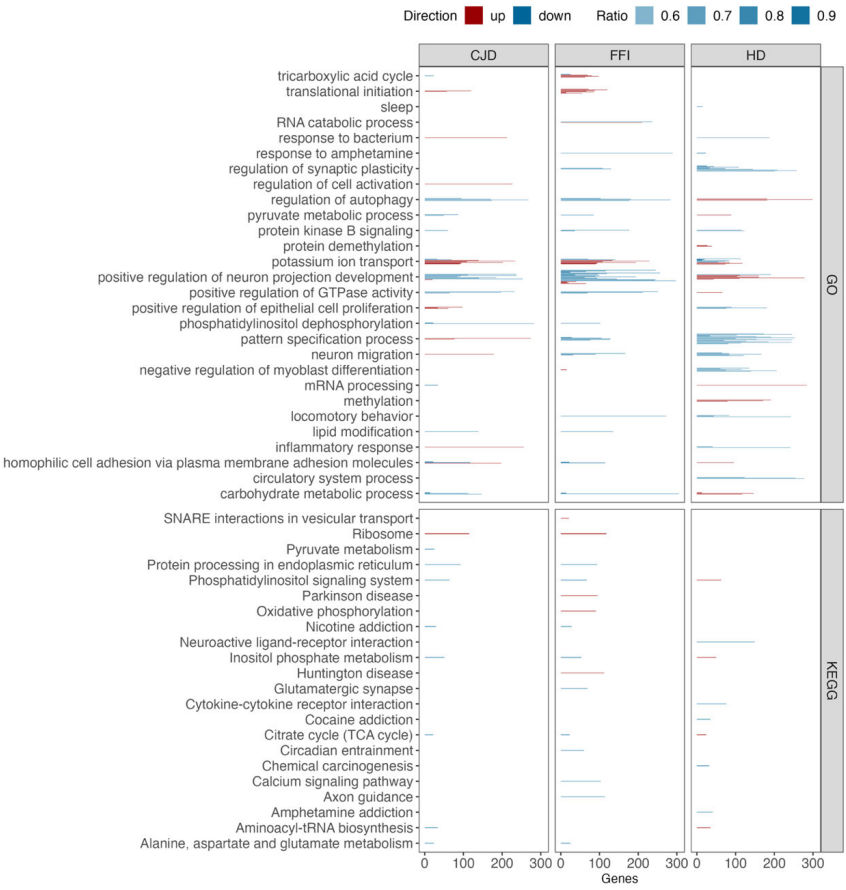

Figure 9: GSEA indicates disease-specific responses in PV^+ neurons. X-axis = the number of included genes. Ratio = included genes/total genes in the set. GO terms were summarized under parent terms by semantic similarity (Resnik, 0.85).

In contrast to our earlier findings, this analysis of a larger data set demonstrated that PV^+ neurons do show a response in the early stages of prion diseases. Our findings were largely in agreement with earlier results from functional analysis but also indicated differences between gCJD, FFI, and HD. Overall, FFI and gCJD also showed some overlap in DEGs, which may indicate that PV^+ neurons show an overall more similar response in prion diseases compared to HD.

Paper IV

Comparative Analysis of Potential Genomic Safe Harbors for Stable Transgene Expression

In mouse models previously developed in our lab[170] we used the *Rosa26* locus[171] for transgene expression, which is generally considered a genomic safe harbor, ideal for ubiquitous and constitutive transgene expression. However, we have previously found that while the Tagger transgene can be successfully expressed in neurons, activation in astrocytes and microglia was poor. This is likely due to variable expression from this locus in mice, especially during early postnatal stages[172,173].

Herein, we conducted a pilot study aiming to investigate the suitability of three loci for expression of the Tagger transgene: *Eef1a1*, *Rpl6*, and *Rpl7*. For each locus, we further compared two different strategies for transgene expression regulation. In the first approach, transgene expression was designed to be driven under control of the TetOff system, with the transactivator domain under the control of the endogenous gene. In the second approach, the transgene was inserted downstream of the 3'UTR under control of the stronger caggs[§] promotor.

Since the goal was to have the new Tagger model in a 129S4 background, we transfected 129S4 (formerly 129Sv/Jae)-derived J1 embryonic stem cells using a CRISPR/Cas9 for site-targeted transgene insertion. Following validation of correct transgene insertion, we found that targeting of the Eef1a1 showed a 21% success rate for the Tet-Off construct but was unsuccessful for the caggs construct. Targeting of the *Rpl6* locus was successful with both strategies (Tet-Off 30%, caggs 5%), but we were not able to obtain successful transgene integration for the *Rpl7* locus. To test whether transgene insertion affected endogenous gene expression, we next quantified the expression of *Rpl6* and *Eef1a1* using ddPCR. This revealed that insertion of the Tet-Off construct reduced the expression of both *Rpl6* and *Eef1a1*, whereas the caggs construct did not reduce *Rpl6* expression, and in fact, slightly increased it.

[§] Also commonly referred to as CAG promotor. To avoid confusion with the CAG trinucleotide repeat, "caggs" was used here.

Concluding Remarks

There is a severe need for therapies for NDs, in part due to an incomplete understanding of disease mechanisms. The problem of selective vulnerability is one example. In this thesis I described work that utilizes existing tools to study cell type-specific responses, and experiments to develop the next generation of tools to uncover even more insights.

To study gene expression changes in pre-symptomatic stages of neurodegenerative diseases we created a novel dataset of cell type-specific translatome data for six cell types in three genetic disease models. Surprisingly, paper I revealed a relatively high number of gene expression changes in SST^+ neurons in both FFI and CJD. While this was intriguing, as SST^+ neurons, though affected in other NDs, were not previously reported to show an early response in prion diseases.

Paper II focused on cell type-specific responses of inhibitory and excitatory cerebellar neurons in pre-symptomatic HD. This indicated a strong response in glutamatergic neurons, which included upregulation of cell cycle regulator *Ccnd1*. We hypothesized these results may be indicative of aberrant cell cycle regulation or dedifferentiation in granular neurons, though further validation is required to test this theory.

Early vulnerability of PV-expressing neurons had been reported in all three investigated diseases. In paper III, we therefore compared disease-specific responses in these neurons, pooling data obtained for papers I and II. Preliminary results indicated the activation of different pathways between the diseases.

The pilot study described in paper IV indicated that of the three investigated loci, *Rpl6* has so far shown the most promising results, as we were able to achieve successful integration of the transgene without negative effects on endogenous gene expression. However, this is based on one data point and further experiments are required to validate these findings. Additionally, while we found that integration did not yield negative effects, we have not yet tested the expression of the Tagger transgene from this locus.

We were surprised to find that in both paper I and paper II, we observed the strongest responses -in terms of the number of DEGs- in cell types that are not commonly reported to be selectively vulnerable. Indeed, previous reports indicate that granular neurons are relatively resistant in HD, compared to Purkinje cells. This left us to speculate whether this early response of *bonafide* resistant neurons constitutes an adaptive response allowing these cells to better cope with the presence of misfolded protein.

As previously addressed, the RiboTag method has several limitations. A limiting factor in our experimental design is a lack of positional information. While we analyzed the cerebrum and cerebellum separately, due to limited resources we did not attempt to further dissect individual brain regions, considering the high costs of both, sample preparation with RiboTag IP and sequencing. As a result, our cell type-specific samples encompass a great variety of smaller

subpopulations, in particular for cerebral cell types, which likely show differences in their gene expression changes. Spatial transcriptomics could be used to analyze expression changes in addition to providing positional information on where in the brain these changes occur.

We hypothesize that one reason why we observed comparatively many DEGs in PV^+ and SST^+ samples is that neuron populations captured in these samples are more homogeneous compared to general GABAergic or glutamatergic populations. As a result, changes originating from a subfraction of targeted neurons are less "diluted" and more likely to be detected in our experiments. However, while this may be a partial explanation for the strong responses, we observed in SST^+ neurons in paper I and cerebellar $vGluT2^+$ neurons in paper II, it is not likely that these findings are mostly artifacts, as in this case, we would have expected a comparable response in cerebellar vGluT2 neurons also in CJD and FFI.

Overall, these studies provided novel and important insights into cell type-specific gene expression changes in pre-symptomatic prion and Huntington's disease. For genetic prion diseases in particular, information at this level of regional and cellular resolution was previously not available. In studies I and II, we chose to focus our attention on cell types that we found were previously under-investigated in the respective diseases. Consequently, we have left numerous other observed responses unexplored, and it is our sincere hope that the dataset generated as part of this thesis will be of further use to the wider research community.

Acknowledgments

Many people have supported me during my time as a Ph.D. student and in the writing of this thesis, be it through scientific, technical, administrative, or mental support. This would not have been possible without you.
Special thanks goes to:

My main supervisor Walker Jackson: Thank you for always having an open door and taking the time whenever I wanted to discuss problems or results with you.

My co-supervisors Martin Hallbeck and Per Hammarström: Thank you for your support through the last 4 years and the interesting scientific discussions during our joint lab meetings.

My colleagues and lab mates:
Maria Jonson: It was always a pleasure to work with you. Thank you for your help and advice, be it on scientific matters or others, and for all the fun days we had in the lab.
Srivathsa Magadi: Thank you for always having the time to talk and for all the interesting discussions about science and life.
Chwen-Yu (John) Chen: Thanks for all your help and sharing your help with the HD project.
Lech Kaczmarckzyk: Thank you for all your help throughout the years and your advice on the data analysis.

Rui Benfeitas: Thank you for the invaluable help during these years, I'm glad to have had you as my mentor.

Lovisa, Juan, Sarah, Cornelia, Aneta, Malin, Sallam, Franciele, David, Anna, Alexander, and all other current and former colleagues on floor 10: I will miss all our fun discussion during lunch or fika and our afterworks. And I'm grateful to have had such great coworkers.

Many thanks also to the organizers, mentors, and fellow mentees at the NBIS Bioinformatics Advisory Program, to all the people working at the LiU Core Facility

And on the personal side:

My husband, Boris: Thank you for being there for me throughout this crazy time, for bringing me countless cups of coffee, for celebrating the successes with me, and for not allowing the setbacks to bring me down. And to our dog, Torro, for keeping me sane by making me leave my computer to go stalk some rabbits.

My parents Harald and Corinna: This would not have been possible without your support and encouragement during all these years. Thank you.

My parents-in-law, Silva and Tomislav: Thank you for your support and help over the years.

My friends and extended family in Sweden and Germany, in particular Georgia, Sophie, Joan, Anita, Gosia, Awais, Diego and Charlotte, Debbie and Jakob. Und die "Wormser", Annette and Tobi R, Jana and Christian, Vanny, Fabian and Daniel, Tobi K, Sabrina and Tobi G.

It has been difficult to catch up with you as often as I would have liked to, but seeing you always takes me right back to the good old times.

References

1. Socialstyrelsen. En nationell strategi för demenssjukdom. (2017).
2. Scheckel, C. & Aguzzi, A. Prions, prionoids and protein misfolding disorders. *Nat. Rev. Genet.* **19**, 405–418 (2018).
3. Fu, H., Hardy, J. & Duff, K. E. Selective vulnerability in neurodegenerative diseases. *Nat. Neurosci.* **21**, 1350–1358 (2018).
4. Deng, Y. P. *et al.* Differential loss of striatal projection systems in Huntington's disease: A quantitative immunohistochemical study. *J. Chem. Neuroanat.* **27**, 143–164 (2004).
5. Reiner, A. *et al.* Differential loss of striatal projection neurons in Huntington disease. *Proc. Natl. Acad. Sci. U. S. A.* **85**, 5733–5737 (1988).
6. Kelly, S. C. *et al.* Locus coeruleus cellular and molecular pathology during the progression of Alzheimer's disease. *Acta Neuropathol. Commun.* **5**, 8 (2017).
7. Lee, H. *et al.* Multi-omic analysis of selectively vulnerable motor neuron subtypes implicates altered lipid metabolism in ALS. *Nat. Neurosci.* **24**, 1673–1685 (2021).
8. Vonsattel, J. P. *et al.* Neuropathological classification of huntington's disease. *J. Neuropathol. Exp. Neurol.* **44**, 559–577 (1985).
9. Sherrington, R. *et al.* Alzheimer's disease associated with mutations in presenilin 2 is rare and variably penetrant. *Hum. Mol. Genet.* **5**, 985–988 (1996).
10. Goate, A. Segregation of a missense mutation in the amyloid β-protein precursor gene with familial Alzheimer's disease. *J. Alzheimer's Dis.* **9**, 341–347 (2006).
11. Chen, W. J. *et al.* Rethinking monogenic neurological diseases. *BMJ* **371**, 9–11 (2020).
12. Papapetropoulos, S., Adi, N., Ellul, J., Argyriou, A. A. & Chroni, E. A prospective study of familial versus sporadic Parkinson's disease. *Neurodegener. Dis.* **4**, 424–427 (2007).
13. Joshi, A., Ringman, J. M., Lee, A. S., Juarez, K. O. & Mendez, M. F. Comparison of clinical characteristics between familial and non-familial early onset Alzheimer's disease. *J. Neurol.* **259**, 2182–2188 (2012).
14. Benussi, A. *et al.* Differences and similarities between familial and sporadic frontotemporal dementia: An Italian single-center cohort study. *Alzheimer's Dement. Transl. Res. Clin. Interv.* **8**, 1–10 (2022).
15. Migliorati, J. M. *et al.* Absorption, Distribution, Metabolism, and Excretion of US Food and Drug Administration–Approved Antisense Oligonucleotide Drugs. *Drug Metab. Dispos.* **50**, 888–897 (2022).
16. Minikel, E. V. *et al.* Prion protein lowering is a disease-modifying therapy across prion disease stages, strains and endpoints. *Nucleic Acids Res.* **48**, 10615–10631 (2020).
17. Walker, F. O. Huntington's disease. *Lancet* **369**, 218–228 (2007).
18. Jacobs, M. *et al.* Progression of motor subtypes in Huntington's disease: a 6-year follow-up study. *J. Neurol.* **263**, 2080–2085 (2016).
19. Lee, J. M. *et al.* CAG Repeat Not Polyglutamine Length Determines Timing of Huntington's Disease Onset. *Cell* **178**, 887-900.e14 (2019).
20. Djoussé, L. *et al.* Interaction of normal and expanded CAG repeat sizes influences age at onset of Huntington disease. *Am. J. Med. Genet.* **119 A**, 279–282 (2003).
21. Ciosi, M. *et al.* A genetic association study of glutamine-encoding DNA sequence structures, somatic CAG expansion, and DNA repair gene variants, with Huntington disease clinical outcomes. *EBioMedicine* **48**, 568–580 (2019).
22. Pinto, R. M. *et al.* Mismatch Repair Genes Mlh1 and Mlh3 Modify CAG Instability in Huntington's Disease Mice: Genome-Wide and Candidate Approaches. *PLoS Genet.* **9**, (2013).
23. Goold, R. *et al.* Article FAN1 controls mismatch repair complex assembly via MLH1 retention to stabilize CAG repeat expansion in Huntington ' s disease ll ll FAN1 controls mismatch repair complex assembly via MLH1 retention to stabilize CAG repeat expansion in Huntington '. (2021) doi:10.1016/j.celrep.2021.109649.
24. Telenius, H. *et al.* Somatic and gonadal mosaicism of the Huntington disease gene CAG repeat in brain and sperm. *Nat. Genet.* **6**, 409–414 (1994).
25. Kaplan, S., Itzkovitz, S. & Shapiro, E. A Universal Mechanism Ties Genotype to Phenotype in Trinucleotide Diseases. **3**, (2007).
26. Culver, B. P. *et al.* Proteomic analysis of wild-type and mutant huntingtin-associated proteins in mouse brains identifies unique interactions and involvement in protein synthesis. *J. Biol. Chem.*

287, 21599–21614 (2012).
27. Saudou, F. & Humbert, S. The Biology of Huntingtin. *Neuron* **89**, 910–926 (2016).
28. Zuccato, C. *et al.* Huntingtin interacts with REST/NRSF to modulate the transcription of NRSE-controlled neuronal genes. *Nat. Genet.* **35**, 76–83 (2003).
29. Seong, I. S. *et al.* Huntingtin facilitates polycomb repressive complex 2. *Hum. Mol. Genet.* **19**, 573–583 (2009).
30. Von Schimmelmann, M. *et al.* Polycomb repressive complex 2 (PRC2) silences genes responsible for neurodegeneration. *Nat. Neurosci.* **19**, 1321–1330 (2016).
31. Malla, B., Guo, X., Senger, G., Chasapopoulou, Z. & Yildirim, F. A Systematic Review of Transcriptional Dysregulation in Huntington's Disease Studied by RNA Sequencing. *Front. Genet.* **12**, 1–22 (2021).
32. Malaiya, S. *et al.* Single-Nucleus RNA-Seq Reveals Dysregulation of Striatal Cell Identity Due to Huntington's Disease Mutations. *J. Neurosci.* **41**, 5334–5352 (2021).
33. Nasir, J. *et al.* Targeted disruption of the Huntington's disease gene results in embryonic lethality and behavioral and morphological changes in heterozygotes. *Cell* **81**, 811–823 (1995).
34. Zeitlin, S., Liu, J., Chapman, D. L. & Papaioannou, V. E. article nullizygous for the Huntington ' s disease gene homo logue. **11**, 155–163 (1995).
35. Barnat, M. *et al.* Huntington's disease alters human neurodevelopment. *Science* **369**, 787–793 (2020).
36. Tereshchenko, A. V *et al.* Abnormal development of cerebellar-striatal circuitry in Huntington disease. *Neurology* **94**, e1908 LP-e1915 (2020).
37. Lee, J. K. *et al.* Measures of growth in children at risk for Huntington disease. *Neurology* **79**, 668 LP – 674 (2012).
38. Godin, J. D. *et al.* Huntingtin Is Required for Mitotic Spindle Orientation and Mammalian Neurogenesis. *Neuron* **67**, 392–406 (2010).
39. McKinstry, S. U. *et al.* Huntingtin is required for normal excitatory synapse development in cortical and striatal circuits. *J. Neurosci.* **34**, 9455–9472 (2014).
40. Mehler, M. F. *et al.* Loss-of-huntingtin in medial and lateral ganglionic lineages differentially disrupts regional interneuron and projection neuron subtypes and promotes huntington's disease-associated behavioral, cellular, and pathological hallmarks. *J. Neurosci.* **39**, 1892–1909 (2019).
41. Albin, R. L. *et al.* Preferential loss of striato-external pallidal projection neurons in presymptomatic Huntington's disease. *Ann. Neurol.* **31**, 425–430 (1992).
42. Arrasate, M., Mitra, S., Schweitzer, E. S., Segal, M. R. & Finkbeiner, S. Inclusion body formation reduces levels of mutant huntingtin and the risk of neuronal death. *Nature* **431**, 805–810 (2004).
43. Arrasate, M. & Finkbeiner, S. Protein aggregates in Huntington's disease. *Exp. Neurol.* **238**, 1–11 (2012).
44. Rüb, U. *et al.* Huntington's disease (HD): the neuropathology of a multisystem neurodegenerative disorder of the human brain. *Brain Pathol.* **26**, 726–740 (2016).
45. Rüb, U. *et al.* Degeneration of the cerebellum in huntingtons disease (HD): Possible relevance for the clinical picture and potential gateway to pathological mechanisms of the disease process. *Brain Pathol.* **23**, 165–177 (2013).
46. Rosas, H. D., Koroshetz, W. J., Chen, Y. I., Skeuse, C. & Vangel, M. Evidence for more widespread cerebral pathology in early HD An MRI-based morphometric analysis. **20**, (2003).
47. Langfelder, P. *et al.* Integrated genomics and proteomics define huntingtin CAG length-dependent networks in mice. *Nat. Neurosci.* **19**, 623–633 (2016).
48. Lee, H. *et al.* Cell Type-Specific Transcriptomics Reveals that Mutant Huntingtin Leads to Mitochondrial RNA Release and Neuronal Innate Immune Activation. *Neuron* **107**, 891-908.e8 (2020).
49. Fossale, E. *et al.* Differential effects of the huntington's disease CAG mutation in striatum and cerebellum are quantitative not qualitative. *Hum. Mol. Genet.* **20**, 4258–4267 (2011).
50. Franklin, G. L., Camargo, C. H. F., Meira, A. T., Lima, N. S. C. & Teive, H. A. G. The Role of the Cerebellum in Huntington's Disease: a Systematic Review. *Cerebellum* **20**, 254–265 (2021).
51. Singh-Bains, M. K. *et al.* Cerebellar degeneration correlates with motor symptoms in Huntington disease. *Ann. Neurol.* **85**, 396–405 (2019).
52. Dougherty, S. E., Reeves, J. L., Lesort, M., Detloff, P. J. & Cowell, R. M. Purkinje cell dysfunction and loss in a knock-in mouse model of Huntington Disease. *Exp. Neurol.* **240**, 96–102 (2013).
53. Jeste, D. V, Barban, L. & Parisi, J. Reduced Purkinje cell density in Huntington's disease. *Exp.*

Neurol. **85**, 78–86 (1984).
54. Padron-Rivera, G. *et al.* Cerebellar Degeneration Signature in Huntington's Disease. *Cerebellum* **20**, 942–945 (2021).
55. Franklin, G. L. *et al.* Is Ataxia an Underestimated Symptom of Huntington's Disease? *Front. Neurol.* **11**, 1–6 (2020).
56. Wu, T. & Hallett, M. The cerebellum in Parkinson's disease. 696–709 (2013) doi:10.1093/brain/aws360.
57. Van Der Plas, E., Schultz, J. L. & Nopoulos, P. C. The Neurodevelopmental Hypothesis of Huntington's Disease. *J. Huntingtons. Dis.* **9**, 217–229 (2020).
58. Moore, R. C. *et al.* Double replacement gene targeting for the production of a series of mouse strains with different prion protein gene alterations. *Biotechnol. (N Y)* **13**, 999–1004 (1995).
59. Bueler, H. *et al.* Normal development and behaviour of mice lacking the neuronal cell-surface PrP protein. *Nature* **356**, 577–582 (1992).
60. Rossi, D. *et al.* Onset of ataxia and Purkinje cell loss in PrP null mice inversely correlated with Dpl level in brain. *EMBO J* **20**, 694–702 (2001).
61. de Almeida, C. J. G. *et al.* The cellular prion protein modulates phagocytosis and inflammatory response. *J. Leukoc. Biol.* **77**, 238–246 (2005).
62. Matamoros-Angles, A. *et al.* Analysis of co-isogenic prion protein deficient mice reveals behavioral deficits, learning impairment, and enhanced hippocampal excitability. *BMC Biol.* **20**, 1–25 (2022).
63. Kishimoto, Y. *et al.* Impairment of cerebellar long-term depression and GABAergic transmission in prion protein deficient mice ectopically expressing PrPLP/Dpl. *Sci. Rep.* **10**, 1–9 (2020).
64. Nuvolone, M. *et al.* Strictly co-isogenic C57BL/6J-Prnp-/- mice: A rigorous resource for prion science. *J. Exp. Med.* **213**, 313–327 (2016).
65. Nuvolone, M. *et al.* SIRPα polymorphisms, but not the prion protein, control phagocytosis of apoptotic cells. *J. Exp. Med.* **210**, 2539–2552 (2013).
66. Geldermann, H. *et al.* Polymorphic microsatellite sites in the PRNP region point to excess of homozygotes in Creutzfeldt-Jakob disease patients. *Gene* **382**, 66–70 (2006).
67. Nurmi, M. H. *et al.* The normal population distribution of PRNP codon 129 polymorphism. *Acta Neurol. Scand.* **108**, 374–378 (2003).
68. Dyrbye, H., Broholm, H., Dziegiel, M. H. & Laursen, H. The M129V polymorphism of codon 129 in the prion gene (PRNP) in the Danish population. *Eur. J. Epidemiol.* **23**, 23–27 (2008).
69. Minikel, E. V., Vallabh, S. M., Orseth, M. C. & Brandel, J. Age at onset in genetic prion disease and the design of preventive clinical trials. (2019) doi:10.1212/WNL.0000000000007745.
70. Goldgaber, D. *et al.* Mutations in familial Creutzfeldt-Jakob disease and Gerstmann-Sträussler-Scheinker's syndrome. *Exp. Neurol.* **106**, 204–206 (1989).
71. Ladogana, A. & Kovacs, G. G. Chapter 13 - Genetic Creutzfeldt–Jakob disease. in *Human Prion Diseases* (eds. Pocchiari, M. & Manson, J. B. T.-H. of C. N.) vol. 153 219–242 (Elsevier, 2018).
72. Kovács, G. G. *et al.* Genetic prion disease: The EUROCJD experience. *Hum. Genet.* **118**, 166–174 (2005).
73. Kovacs, G. G. *et al.* Genetic Creutzfeldt-Jakob disease associated with the E200K mutation: Characterization of a complex proteinopathy. *Acta Neuropathol.* **121**, 39–57 (2011).
74. Ye, H. *et al.* Thalamic-insomnia phenotype in E200K Creutzfeldt–Jakob disease: A PET/MRI study. *NeuroImage Clin.* **35**, 103086 (2022).
75. Cohen, O. S. *et al.* Familial Creutzfeldt–Jakob disease with the E200K mutation: longitudinal neuroimaging from asymptomatic to symptomatic CJD. *J. Neurol.* **262**, 604–613 (2015).
76. Barriga, F., Ruiz-Dominguez, J. A. & Velayos, J. L. [Familial fatal insomnia: a human prion disease which opens the door to a greater understanding of the thalamus]. *Rev Med Univ Navarra* **41**, 224–228 (1997).
77. Medori, R. *et al.* Fatal familial insomnia, a prion disease with a mutation at codon 178 of the prion protein gene. *N Engl J Med* **326**, 444–449 (1992).
78. Parchi, P. *et al.* Molecular pathology of fatal familial insomnia. *Brain Pathol* **8**, 539–548 (1998).
79. Goldfarb, L. G. *et al.* Fatal familial insomnia and familial Creutzfeldt-Jakob disease: disease phenotype determined by a DNA polymorphism. *Science (80-.).* **258**, 806–808 (1992).
80. Zerr, I. & Schmitz, M. Genetic Prion Disease Summary Genetic counseling GeneReview Scope Suggestive Findings. 1–16 (2023).
81. Baiardi, S. *et al.* Phenotypic diversity of genetic Creutzfeldt–Jakob disease: a histo-molecular-

based classification. *Acta Neuropathol.* **142**, 707–728 (2021).
82. Zhang, J. *et al.* Clinical profile of fatal familial insomnia: phenotypic variation in 129 polymorphisms and geographical regions. *J. Neurol. Neurosurg. Psychiatry* **93**, 291–297 (2022).
83. Montagna, P. *et al.* Clinical features of fatal familial insomnia: phenotypic variability in relation to a polymorphism at codon 129 of the prion protein gene. *Brain Pathol* **8**, 515–520 (1998).
84. Cortelli, P., Gambetti, P., Montagna, P. & Lugaresi, E. Fatal familial insomnia: clinical features and molecular genetics. *J Sleep Res* **8 Suppl 1**, 23–29 (1999).
85. Llorens, F. *et al.* Identification of new molecular alterations in fatal familial insomnia. *Hum Mol Genet* **25**, 2417–2436 (2016).
86. Shi, Q. *et al.* Brain microglia were activated in sporadic CJD but almost unchanged in fatal familial insomnia and G114V genetic CJD. *Virol. J.* **10**, 1–9 (2013).
87. Tian, C. *et al.* Comparative analysis of gene expression profiles between cortex and thalamus in chinese fatal familial insomnia patients. *Mol. Neurobiol.* **48**, 36–48 (2013).
88. Frau-Méndez, M. A. *et al.* Fatal familial insomnia: mitochondrial and protein synthesis machinery decline in the mediodorsal thalamus. *Brain Pathol.* **27**, 95–106 (2017).
89. Shi, Q. *et al.* Proteomics analyses for the global proteins in the brain tissues of different human prion diseases. *Mol. Cell. Proteomics* **14**, 854–869 (2015).
90. Vong, L. *et al.* Leptin action on GABAergic neurons prevents obesity and reduces inhibitory tone to POMC neurons. *Neuron* **71**, 142–154 (2011).
91. Herzog, E., Takamori, S., Jahn, R., Brose, N. & Wojcik, S. M. Synaptic and vesicular co-localization of the glutamate transporters VGLUT1 and VGLUT2 in the mouse hippocampus. *J. Neurochem.* **99**, 1011–1018 (2006).
92. Miyazaki, T., Fukaya, M., Shimizu, H. & Watanabe, M. Subtype switching of vesicular glutamate transporters at parallel fibre–Purkinje cell synapses in developing mouse cerebellum. *Eur. J. Neurosci.* **17**, 2563–2572 (2003).
93. Taniguchi, H. *et al.* A Resource of Cre Driver Lines for Genetic Targeting of GABAergic Neurons in Cerebral Cortex. *Neuron* **71**, 995–1013 (2011).
94. Rudy, B., Fishell, G., Lee, S. H. & Hjerling-Leffler, J. Three groups of interneurons account for nearly 100% of neocortical GABAergic neurons. *Dev. Neurobiol.* **71**, 45–61 (2011).
95. Tremblay, R., Lee, S. & Rudy, B. GABAergic Interneurons in the Neocortex: From Cellular Properties to Circuits. *Neuron* **91**, 260–292 (2016).
96. Artinian, J. *et al.* Regulation of hippocampal memory by mTORC1 in somatostatin interneurons. *J. Neurosci.* **39**, 8439–8456 (2019).
97. Kim, D. *et al.* Distinct Roles of Parvalbumin- and Somatostatin-Expressing Interneurons in Working Memory. *Neuron* **92**, 902–915 (2016).
98. Funk, C. M. *et al.* Role of somatostatin-positive cortical interneurons in the generation of sleep slow waves. *J. Neurosci.* **37**, 9132–9148 (2017).
99. Thankachan, S. *et al.* Thalamic Reticular Nucleus Parvalbumin Neurons Regulate Sleep Spindles and Electrophysiological Aspects of Schizophrenia in Mice. *Sci. Rep.* **9**, 1–16 (2019).
100. Reiner, A. *et al.* Striatal parvalbuminergic neurons are lost in Huntington's disease: Implications for dystonia. *Mov. Disord.* **28**, 1691–1699 (2013).
101. Nassar, M. *et al.* Diversity and overlap of parvalbumin and somatostatin expressing interneurons in mouse presubiculum. *Front. Neural Circuits* **9**, 1–19 (2015).
102. Jang, H. J. *et al.* Distinct roles of parvalbumin and somatostatin interneurons in gating the synchronization of spike times in the neocortex. *Sci. Adv.* **6**, (2020).
103. Algamal, M. *et al.* Reduced excitatory neuron activity and interneuron-type-specific deficits in a mouse model of Alzheimer's disease. *Commun. Biol.* **5**, 1–9 (2022).
104. Morrone, C. D., Lai, A. Y., Bishay, J., Hill, M. E. & McLaurin, J. Parvalbumin neuroplasticity compensates for somatostatin impairment, maintaining cognitive function in Alzheimer's disease. *Transl. Neurodegener.* **11**, 26 (2022).
105. Schmid, L. C. *et al.* Dysfunction of Somatostatin-Positive Interneurons Associated with Memory Deficits in an Alzheimer's Disease Model. *Neuron* **92**, 114–125 (2016).
106. Schmid, L. C. *et al.* Dysfunction of Somatostatin-Positive Interneurons Associated with Memory Deficits in an Alzheimer’s Disease Model. *Neuron* **92**, 114–125 (2016).
107. Rallapalle, V., King, A. C. & Gray, M. BACHD Mice Recapitulate the Striatal Parvalbuminergic Interneuron Loss Found in Huntington's Disease. *Front. Neuroanat.* **15**, 1–10 (2021).
108. Holley, S. M., Galvan, L., Kamdjou, T., Cepeda, C. & Levine, M. S. Striatal GABAergic

interneuron dysfunction in the Q175 mouse model of Huntington's disease. *Eur. J. Neurosci.* **49**, 79–93 (2019).
109. Guentchev, M., Wanschitz, J., Voigtlander, T., Flicker, H. & Budka, H. Selective neuronal vulnerability in human prion diseases. Fatal familial insomnia differs from other types of prion diseases. *Am J Pathol* **155**, 1453–1457 (1999).
110. Guentchev, M., Hainfellner, J. A., Trabattoni, G. R. & Budka, H. Distribution of parvalbumin-immunoreactive neurons in brain correlates with hippocampal and temporal cortical pathology in Creutzfeldt-Jakob disease. *J Neuropathol Exp Neurol* **56**, 1119–1124 (1997).
111. Jackson, W. S. *et al.* Spontaneous generation of prion infectivity in fatal familial insomnia knockin mice. *Neuron* **63**, 438–450 (2009).
112. Jackson, W. S. *et al.* Profoundly different prion diseases in knock-in mice carrying single PrP codon substitutions associated with human diseases. *Proc. Natl. Acad. Sci. U. S. A.* **110**, 14759–14764 (2013).
113. Lin, C. H. *et al.* Neurological abnormalities in a knock-in mouse model of Huntington's disease. *Hum Mol Genet* **10**, 137–144 (2001).
114. Heng, M. Y. *et al.* Early autophagic response in a novel knock-in model of Huntington disease. *Hum. Mol. Genet.* **19**, 3702–3720 (2010).
115. Kaczmarczyk, L. *et al.* Slc1a3-2A-CreERT2 mice reveal unique features of Bergmann glia and augment a growing collection of Cre drivers and effectors in the 129S4 genetic background . *Sci Rep* **11**, 5412 (2021).
116. Sanz, E. *et al.* Cell-type-specific isolation of ribosome-associated mRNA from complex tissues. *Proc. Natl. Acad. Sci. U. S. A.* **106**, 13939–13944 (2009).
117. Sanz, E., Bean, J. C., Carey, D. P., Quintana, A. & McKnight, G. S. RiboTag: Ribosomal Tagging Strategy to Analyze Cell-Type-Specific mRNA Expression In Vivo. *Curr. Protoc. Neurosci.* **88**, e77 (2019).
118. Sauer, B. Inducible Gene Targeting in Mice Using the Cre/loxSystem. *Methods* **14**, 381–392 (1998).
119. Heiman, M. *et al.* A translational profiling approach for the molecular characterization of CNS cell types. *Cell* **135**, 738–748 (2008).
120. Jung, J. & Jung, H. Methods to analyze cell type-specific gene expression profiles from heterogeneous cell populations. *Animal Cells Syst. (Seoul).* **20**, 113–117 (2016).
121. Macosko, E. Z. *et al.* Highly parallel genome-wide expression profiling of individual cells using nanoliter droplets. *Cell* **161**, 1202–1214 (2015).
122. Manuelidis, L. Decontamination of Creutzfeldt-Jakob Disease and other transmissible agents. *J. Neurovirol.* **3**, 62–65 (1997).
123. Ewels, P. A. *et al.* The nf-core framework for community-curated bioinformatics pipelines. *Nature biotechnology* vol. 38 276–278 (2020).
124. Patel, H. *et al.* nf-core/rnaseq: nf-core/rnaseq v3.10.1 - Plastered Rhodium Rudolph. (2023) doi:10.5281/ZENODO.7505987.
125. Patro, R., Duggal, G., Love, M. I., Irizarry, R. A. & Kingsford, C. Salmon provides fast and bias-aware quantification of transcript expression. *Nat. Methods* **14**, 417–419 (2017).
126. Love, M. I., Huber, W. & Anders, S. Moderated estimation of fold change and dispersion for RNA-seq data with DESeq2. *Genome Biol.* **15**, 550 (2014).
127. Kanehisa, M. & Goto, S. KEGG: Kyoto Encyclopedia of Genes and Genomes. *Nucleic Acids Res.* **28**, 27–30 (2000).
128. Kanehisa, M. Toward understanding the origin and evolution of cellular organisms. *Protein Sci.* **28**, 1947–1951 (2019).
129. Ashburner, M. *et al.* Gene Ontology: tool for the unification of biology. *Nat. Genet.* **25**, 25–29 (2000).
130. Thomas, P. D. The Gene Ontology and the Meaning of Biological Function BT - The Gene Ontology Handbook. in (eds. Dessimoz, C. & Škunca, N.) 15–24 (Springer New York, 2017). doi:10.1007/978-1-4939-3743-1_2.
131. Supek, F., Bošnjak, M., Škunca, N. & Šmuc, T. REVIGO Summarizes and Visualizes Long Lists of Gene Ontology Terms. *PLoS One* **6**, e21800 (2011).
132. Chen, E. Y. *et al.* Enrichr: interactive and collaborative HTML5 gene list enrichment analysis tool. *BMC Bioinformatics* **14**, 128 (2013).
133. Lachmann, A. *et al.* ChEA: Transcription factor regulation inferred from integrating genome-wide

ChIP-X experiments. *Bioinformatics* **26**, 2438–2444 (2010).
134. Subramanian, A. *et al.* Gene set enrichment analysis: A knowledge-based approach for interpreting genome-wide expression profiles. *Proc. Natl. Acad. Sci.* **102**, 15545 LP – 15550 (2005).
135. Mootha, V. K. *et al.* PGC-1α-responsive genes involved in oxidative phosphorylation are coordinately downregulated in human diabetes. *Nat. Genet.* **34**, 267–273 (2003).
136. Maciejewski, H. Gene set analysis methods: statistical models and methodological differences. *Brief. Bioinform.* **15**, 504–518 (2014).
137. Väremo, L., Nielsen, J. & Nookaew, I. Enriching the gene set analysis of genome-wide data by incorporating directionality of gene expression and combining statistical hypotheses and methods. *Nucleic Acids Res.* **41**, 4378–4391 (2013).
138. Montenegro, J. D. Gene Co-expression Network Analysis BT - Plant Bioinformatics: Methods and Protocols. in (ed. Edwards, D.) 387–404 (Springer US, 2022). doi:10.1007/978-1-0716-2067-0_19.
139. Langfelder, P. & Horvath, S. WGCNA: An R package for weighted correlation network analysis. *BMC Bioinformatics* **9**, (2008).
140. Barabási, A.-L., Gulbahce, N. & Loscalzo, J. Network medicine: a network-based approach to human disease. *Nat. Rev. Genet.* **12**, 56–68 (2011).
141. Traag, V. A., Waltman, L. & van Eck, N. J. From Louvain to Leiden: guaranteeing well-connected communities. *Sci. Rep.* **9**, 1–12 (2019).
142. Wang, F. *et al.* RNAscope: A novel in situ RNA analysis platform for formalin-fixed, paraffin-embedded tissues. *J. Mol. Diagnostics* **14**, 22–29 (2012).
143. Li, E., Bestor, T. H. & Jaenisch, R. Targeted mutation of the DNA methyltransferase gene results in embryonic lethality. *Cell* **69**, 915–926 (1992).
144. Klofas, L. K. *et al.* DEPDC5 haploinsufficiency drives increased mTORC1 signaling and abnormal morphology in human iPSC-derived cortical neurons. *Neurobiol. Dis.* **143**, 104975 (2020).
145. Xie, W. *et al.* The chromatin remodeling complex NuRD establishes the poised state of rRNA genes characterized by bivalent histone modifications and altered nucleosome positions. *Proc. Natl. Acad. Sci. U. S. A.* **109**, 8161–8166 (2012).
146. Rolicka, A. *et al.* The chromatin-remodeling complexes B-WICH and NuRD regulate ribosomal transcription in response to glucose. *FASEB J.* **34**, 10818–10834 (2020).
147. Perluigi, M., Di Domenico, F. & Butterfield, D. A. mTOR signaling in aging and neurodegeneration: At the crossroad between metabolism dysfunction and impairment of autophagy. *Neurobiol. Dis.* **84**, 39–49 (2015).
148. Delarue, M. *et al.* mTORC1 Controls Phase Separation and the Biophysical Properties of the Cytoplasm by Tuning Crowding. *Cell* **174**, 338-349.e20 (2018).
149. Terenzio, M. *et al.* Locally translated mTOR controls axonal local translation in nerve injury. *Science (80-.).* **359**, 1416–1421 (2018).
150. Querfurth, H. & Lee, H. K. Mammalian/mechanistic target of rapamycin (mTOR) complexes in neurodegeneration. *Mol. Neurodegener.* **16**, 1–25 (2021).
151. Xu, Y. *et al.* Activation of the macroautophagic system in scrapie-infected experimental animals and human genetic prion diseases. *Autophagy* **8**, 1604–1620 (2012).
152. Zhou, X., Liao, W. J., Liao, J. M., Liao, P. & Lu, H. Ribosomal proteins: Functions beyond the ribosome. *J. Mol. Cell Biol.* **7**, 92–104 (2015).
153. Tereshchenko, A. V. *et al.* Abnormal development of cerebellar-striatal circuitry in Huntington disease. *Neurology* **94**, e1908–e1915 (2020).
154. Chauhan, M., Modi, P. K. & Sharma, P. Aberrant activation of neuronal cell cycle caused by dysregulation of ubiquitin ligase Itch results in neurodegeneration. *Cell Death Dis.* **11**, 1–13 (2020).
155. Marathe, S., Liu, S., Brai, E., Kaczarowski, M. & Alberi, L. Notch signaling in response to excitotoxicity induces neurodegeneration via erroneous cell cycle reentry. *Cell Death Differ.* **22**, 1775–1784 (2015).
156. Dietrich, P. *et al.* Identification of cyclin D1 as a major modulator of 3-nitropropionic acid-induced striatal neurodegeneration. *Neurobiol. Dis.* **162**, 105581 (2022).
157. Modi, P. K., Komaravelli, N., Singh, N. & Sharma, P. Interplay between MEK-ERK signaling, cyclin D1, and cyclin-dependent kinase 5 regulates cell cycle reentry and apoptosis of neurons. *Mol. Biol. Cell* **23**, 3722–3730 (2012).
158. Zhao, A. *et al.* Overexpression of cyclin D1 induces the reprogramming of differentiated epidermal cells into stem cell-like cells. *Cell Cycle* **15**, 644–653 (2016).

159. Caldwell, A. B. *et al.* Dedifferentiation and neuronal repression define familial Alzheimer's disease. *Sci. Adv.* **6**, (2020).
160. Mertens, J. *et al.* Age-dependent instability of mature neuronal fate in induced neurons from Alzheimer's patients. *Cell Stem Cell* 1533–1548 (2021) doi:10.1016/j.stem.2021.04.004.
161. Ismail, I. H. *et al.* CBX4-mediated SUMO modification regulates BMI1 recruitment at sites of DNA damage. *Nucleic Acids Res.* **40**, 5497–5510 (2012).
162. Ren, X. & Kerppola, T. K. REST Interacts with Cbx Proteins and Regulates Polycomb Repressive Complex 1 Occupancy at RE1 Elements. *Mol. Cell. Biol.* **31**, 2100–2110 (2011).
163. Deacon, R. M. Burrowing in rodents: a sensitive method for detecting behavioral dysfunction. *Nat Protoc* **1**, 118–121 (2006).
164. Dougherty, S. E. *et al.* Hyperactivity and cortical disinhibition in mice with restricted expression of mutant huntingtin to parvalbumin-positive cells. *Neurobiol. Dis.* **62**, 160–171 (2014).
165. Ferrer, I., Casas, R. & Rivera, R. Parvalbumin-immunoreactive cortical neurons in Creutzfeldt-Jakob disease. *Ann Neurol* **34**, 864–866 (1993).
166. Albin, R. L., Reiner, A., Anderson, K. D., Penney, J. B. & Young, A. B. Striatal and nigral neuron subpopulations in rigid Huntington's disease: implications for the functional anatomy of chorea and rigidity-akinesia. *Ann. Neurol.* **27**, 357–365 (1990).
167. Belichenko, P. V, Miklossy, J., Belser, B., Budka, H. & Celio, M. R. Early destruction of the extracellular matrix around parvalbumin-immunoreactive interneurons in Creutzfeldt-Jakob disease. *Neurobiol Dis* **6**, 269–279 (1999).
168. Guentchev, M., Wanschitz, J., Voigtländer, T., Flicker, H. & Budka, H. Selective neuronal vulnerability in human prion diseases: Fatal familial insomnia differs from other types of prion diseases. *Am. J. Pathol.* **155**, 1453–1457 (1999).
169. Areškevičiūtė, A. *et al.* Regional differences in neuroinflammation-associated gene expression in the brain of sporadic creutzfeldt–jakob disease patients. *Int. J. Mol. Sci.* **22**, 1–17 (2021).
170. Kaczmarczyk, L. *et al.* Tagger-A Swiss army knife for multiomics to dissect cell type-specific mechanisms of gene expression in mice. *PLoS Biol.* **17**, e3000374 (2019).
171. Friedrich, G. & Soriano, P. Promoter traps in embryonic stem cells: A genetic screen to identify and mutate developmental genes in mice. *Genes Dev.* **5**, 1513–1523 (1991).
172. Clarke, L. E. *et al.* Normal aging induces A1-like astrocyte reactivity. *Proc. Natl. Acad. Sci. U. S. A.* **115**, E1896–E1905 (2018).
173. Shin, S. *et al.* Comprehensive Analysis of Genomic Safe Harbors as Target Sites for Stable Expression of the Heterologous Gene in HEK293 Cells. *ACS Synth. Biol.* **9**, 1263–1269 (2020).

FACULTY OF MEDICINE AND HEALTH SCIENCES

Linköping University Medical Dissertation Nr. 1852, 2023
Department of Biomedical and Clinical Sciences

Linköping University
SE-581 83 Linköping, Sweden

www.liu.se

LINKÖPING UNIVERSITY